بسم الله الرحمن الرحيم

Sudan University of Science and Technology

College of Petroleum Engineering and Mining

Department of Petroleum Exploration engineering

Graduation research to take BSc degree in Petroleum Exploration Engineering

Petrophysical Characterization of shaly sandstone reservoirs in Jake-South oil field Muglad basin, Sudan

الخصائص البتروفيزيائية لمكامن الطفل الرملية في حقل (Jake-South) في حوض المجلد في السودان

Prepared by:

1. Adam Mohammed Ahmed Dafa Alla

2.Babiker Alhassan Mohammed Ali Mohamed

3.Buraei Mohammed Al Helo Eid

4.Mazin Abdalhameed Ismael Mohammed

Supervisor: **T. Amro Yusuf**

October/ 2020

الإهـــداء

الى من كلت أناملة ليقدم لنا لحظة سعادة

الى من حصدوا الاشواك عن دروبنا ليمهد لنا طريق العلم

الى رمز الحب و بلسم الشفاء

شكر و تقدير

الى من أخلصت النية في التعليم فنورت عقولنا

و هذبت نفوسنا و ربيت اجيالاً الى السراج

الذي يحرق نفسه لينير الطريق لغيره

Abstract

Water saturation estimation by interpretation of Archie's model in clean formations has successfully been used over the years. However, due to shale or clay effects in shaly sand formation this model results in inaccurate water saturation values. Many shaly sand interpretation models have been developed, unfortunately there is no unique model that appears to fit all shaly sand reservoirs. A comparison study of water saturations on wells Jake-south (28, 34, 37and S2) was carried out using three different saturation models (Archie, Indonesian, Simandoux). The entire interpretation was done using the Interactive Petro physics Software. Formation permeability was estimated using porosity – permeability relationship derived from core measurement. The results from the study have shown that the average water saturation values from Archie model ranges from (16% - 28%) were higher than that of simandoux models. The result from the Simandoux model is (8% - 20%). The Indonesian model yields average water saturation value is (18% - 32%) which is close to that given by Archie model and higher than the value of the Simandoux model. Indonesian model is the most optimistic for the study after the correlation of all models with the core data given. Sub zones bearing commercial hydrocarbon were identified by determining their porosity, permeability, oil saturation and the hydrocarbon mobility index.

التجريد

تم استخدام نموذج *Archie* في حساب تشبعات المياه في التكاوين الرمليه وكانت مفيدة بصورة جلية . ومع ذلك ، في التكاوين الطينيه الرمليه قد يكون هذا النموذج غير دقيق في النتائج بسبب تاثير الطين . تم تطوير العديد من النماذج لتفسير التكاوين الطينيه الرمليه ، ولكن لا يوجد نموذج معين قد اثبت فاعليته لكي يناسب جميع الخزانات الطينيه الرمليه و أجريت دراسات لمقارنة تشبعات المياه على الآبار *Jake-south (28 , 34 , 37 , s2)* باستخدام ثلاثة نماذج مختلفة لحساب تشبع المياه (*Archie*،*Simandoux*, *Indonesian*) وبالتالي تم التفسير الكامل باستخدام برنامج *Interactive petro physics*تم تقدير نفاذيه التكوين عن طريق العلاقه بين المساميه و النفاذيه الماخوذه من البيانات المعمليه. أظهرت نتائج الدراسة أن متوسط قيم تشبع الماء باستخدام نموذج *Archie* **(16% - 28%)** وكانت أعلى من القيم التي تم التحصل عليها بواسطه نموذج *Simandoux* والتي تتراوح من **(8% - 20%)** بينما القيمة التي تم الحصول عليها عن طريق نموذج *Indonesian*كانت **(18% - 32%)** وهي اعلي من قيمة نموذج *Simandoux* واقرب الي قيمة نموذج *Archie* . وعليه من خلال مقارنة النتائج التي تم التحصل عليها اتضح ان نموذج *Indonesian* هو الأكثر ملائمة في الدراسة وذلك بعد ربطه بالبيانات الأساسية المعطاة .

Table of Contents:

List of Figures:

List of Tables:

Nomenclature:

BHT = Bore hole temperature

To = Surface Temperature

D = Depth

a = tortuosity of the rock, unit less

GR = Gamma ray, API.

IGR = Gamma ray index.

K = Permeability (mD)

m = Cementation exponent, dimensionless

n = Saturation exponent, dimensionless

N-D = Neutron-Density porosity logs.

PHE = Effective porosity from neutron-density logs (v/v).

ϕ = Formation porosity, (v/v).

Rsh = Shale formation resistivity, Ohms-meter.

Rt = Formation resistivity, ohms-meter

Rw = Formation water resistivity, ohms-meter.

SW_AR = Archie water saturation, (v/v).

Swavg = Average water saturation

SW_INDO = Indonesian water saturation, (v/v).

SW_SIM = Simandoux water saturation, (v/v).

Sw = Water saturation

Sxo = Flushed zone water saturation

Rmf = Mud filtrate Resistivity

ØD = Density Porosity

ØDsh = Density Porosity in shale formations

Øe = Effective Porosity

ØN = Neutron Porosity

ØNsh = Neutron Porosity in shale formatio

CHAPTER 1

Introduction

1.1 Overview:

Many reservoirs especially the clastic reservoirs contain quite often a little amount of clays and shales as probably well-known those components have an effect not only on porosity and permeability but on density, neutron, sonic, resistivity and gamma ray log responses. This is related to their own chemical composition and electrical properties consequently it is very important to evaluate very precisely as much as possible their percentage and their distribution inside the reservoir units.

Clay is one of a complex and loosely defined group of finely crystalline metacolloidal or amorphous hydrous silicates essentially of aluminum and sometimes magnetite and iron. The clay effect in shaly sand formations experiments have shown that the conductivity of the oil is much higher than in the clean formation due to the conductivity of the clay, the negative surface charge produced by the structure of the clay minerals is due to the substitution at the surface of the clay crystals of atoms of lower positive valence. The log analyst faces formidable problem when confronted by shaly sand, a discussion is usually made between the term clay and shale in this discussion clay or dry clay will be used to refer to dehydrated clay minerals and shale will be used to refer to hydrated clay materials. In some of the literatures the terms are used interchangeably which can confuse the issue, the shale has effect on response on logging tools according to the distribution of the clay material, type of the clay material, the amount of the clay material, the salinity of the formation water and water saturation. clays are defined as natural earthy fine grained materials that develop plasticity when wet they are formed from chemical weathering of igneous and metamorphic rocks the major source of commercial clays is volcanic ash. Tetrahedral layers these are made of a flat honeycomb sheet of tetrahedral containing a central silicon atoms surrounded by four oxygen’s the tetrahedral are linked to form a sheet by sharing three of their oxygen atoms with adjacent tetrahedral, octahedral layers these are sheets composed of linked octahedral each made up of an aluminum or magnesium atom surrounded by six oxygen’s, again the links are made up by sharing oxygen atoms between two or three

neighboring octahedral and exchangeable layers these are layers of atoms or molecules bound loosely into the structure which can be exchanged with other atoms or molecules these exchangeable atoms or molecules are very important as they give the clays unique physical and chemical properties. The nature of the above layers and the way they are stacked together define the type of clay mineral for this reason they are several types of clays available In the reservoir rock the shale effect one of the controversial problems in formation evaluation the presence of highly radioactive material in shaly sand reservoirs overestimates the shale volume producing and overall pessimistic scenario of the reservoir quality (Schull 1988). An accurate determination of shale volume impacts in the calculation of the formation porosity and water saturation and therefore affects the original oil in place and reserves. The main objective is to estimate the clay and shale effect of petrophysical properties in Siliclastic sandstone reservoir in Muglad basin and the second aim is to calculate the values of petrophysical properties using Archie's model, Indonesian model and Simandoux model make correlation between all this models results and core data to be very unique and accurate.

1.2 Objectives:

1.2.1 Main Objective:

Characterization of clay/shale impact on petrophysical properties' of siliclastic Bentiu sandstone reservoir in Jake south oilfield Muglad basin and identify hydrocarbon mobility by using well logging and comparing the result with the core data, identifying hydrocarbon mobility index and pay zones.

1.2.2 Specific Objectives:

1- Interpretation the lithology obtained by using GR, resistivity and neutron and density logs.

2- Shale Volume determination.

3- Determining total & effective porosities as well as water saturation.

4- Estimation of the permeability from the core values of porosity and permeability cross plot.

1.3 Study area:

The area is located in the southern Sudan in block twenty-three with an area of about 69252Km^2 located within the muglad basin which is one of the major components of the West and Central Africa Rift System (WCARS). The block 23 includes three main sedimentary sub basins Gabgba, Salima and Abyad. The Muglad basin idealizes part of Central Africa Rift System. It is oriented NW-SE. The basin is situated within Sudan and South Sudan, and it covers an area of approximately 120,000 km² (Abdelhakam and Ali 2008). The study area (Jake oilfield) is located on the Western Escarpment of the Fula Sub-basin of the Muglad Basin in Sudan **Figure (1)**. The area is approximately bounded by the latitudes 11°20' and 11°36′ N and longitudes 28° 30′ and 29° 36′ E. This oilfield has been structurally subdivided into three main structures, which are Jake, Jake Central and Jake South.

A total of 44 wells have been drilled in the Jake oilfield. There are four proven hydrocarbon-bearing formations: Ghazal, Zarqa, Bentiu and Abu Gabra, and two producing formations: Bentiu and Abu Gabra.

It's also characterized by low relief flat plain area surrounded by three types of structures and igneous extrusion, in the NW of the basin is bounded by Marra and Nuba mountains in the NE, with the exception of some isolated sandstone outcrops of Miocene to Pliocene age east of the Muglad town. The superficial deposits of black cotton soils cover the area by laterite deposits. Moreover, alluvial and wadi sediments as well as swamp deposits of the White Nile tributaries. The stratigraphy of the study and adjacent areas are ranging from Precambrian to quaternary.

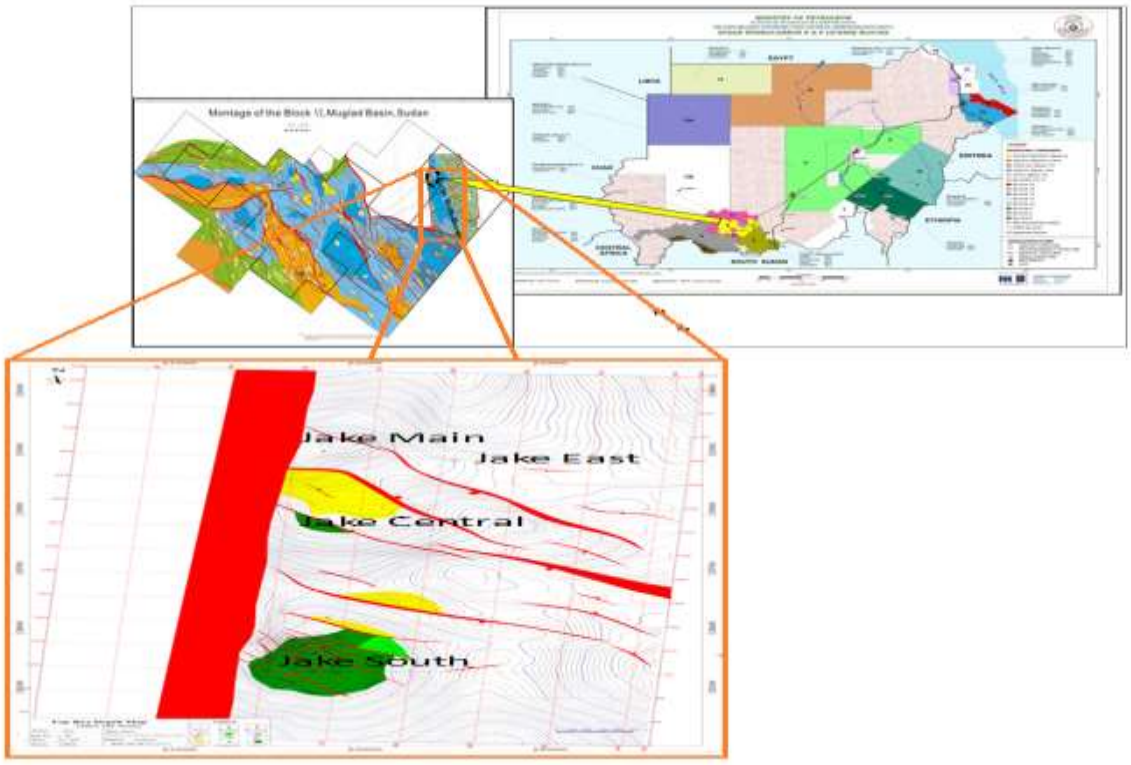

Figure (1) :Location map of Jake oilfield in Fula Sub-Basin, Block-6 of Sudan

1.3.1 Tectonic and Structural Setting:

The development of oil - bearing basins in Sudan is closely associated with the global phenomenon of plate tectonics and particularly with the Africa-South America rifting (Fairhead,1988; Schull, 1988). The rift basins of southern Sudan are related to processes that operated not only within central Africa, but also along the western and eastern continental margins. The Sudanese interior basins are interpreted to be of Mesozoic to Tertiary age, thus the late Jurassic to early Cretaceous Muglad Basin forms part of the West and Central African Rift-System. The basin evolution has been divided into pre-rift and rift phases.

The rifting is divided into three major phases:

- Phase 1 – Late Jurassic Early Cretaceous (140-95 Ma).

- Phase 2 – Late Cretaceous (95-65 Ma).

- Phase 3 – Paleocene (65-30 Ma).

The structural system is characterized by northwest trending faults with different throws with overall NNW-SSE and NW-SE strikes. This trend is possibly area activation of the late Precambrian to Early Paleozoic Pan African Shear Zone. In seismic lines and cross-sections, the faults present planar normal faults and listric normal faults in rotated fault zones. The styles of the structures mainly include rotated tilted fault blocks, faulted anticlines and horst blocks (Schull, 1988). The faults usually juxtapose the sands of the upper Bentiu against Aradeiba shale section. These faults totally control structure evolution, generating oil-trapping fault block and tensional movements resulting in a tilted fault–block structural style marked the early phase in the history of the basin.

Figure (2) :Tectonic models of the West and Central African Rift Systems

1.3.2 Stratigraphy:

The basement adjacent to the Muglad basin is predominantly Precambrian and Cambrian metamorphic rocks with limited occurrences of intrusive igneous rocks. The rock types are mainly metamorphic rocks, which include, granitic gneiss, and granodiorite gneiss.

This gneissic basement is overlain by quartzite of Paleozoic age. From the Cambrian into the Mesozoic, the Muglad basin was the location of an extensive continental platform. The oldest sedimentary rocks are non-marine of lower Jurassic salt (halite), siltstones, and Permo-Triassic clay stones of the Blue Nile basin.

The deepest part of the Muglad basin lies to the west of Unity field, it is estimated to contain over 4500m of Tertiary and 6000 to 9000m of Cretaceous non-marine sediments derived from surrounding basement complex (Fairhead,1988).

The establishment of the stratigraphic column reflects three cycles of deposition in Muglad basin. The Sharef, Abu Gabra, and Bentiu Formations represent the first cycle, second cycle is the Cretaceous of Darfur Group and is characterized by a coarsening upward sequence, and the third one is Nail formation.

The age of these cycles are: -

(a) Late Jurassic to Cenomanian,

(b) Turonian to Paleocene,

(c) Early Tertiary respectively.

Sharif and Abu Gabra Formations:

The early graven-fill clastics are first-cycle sediments derived from the gneissic basement complex. During the early phases of rifting, Neocomian and Barremian clay stones, silt- stones, and fine-grained sandstones of the Sharaf for motion were deposited in fluvial-floodplain and lacustrine environments.

Toward the basin edges and in the areas of major sediment influx these sediments graded to coarse alluvial elastics.

The maximum penetration of this unit is approximately (366 m) in the northwest Muglad basin; however, seismically, the unit is indicated to be much thicker in the deeper troughs. The Aptian early Albian Abu Gabra Formation represents the period of greatest lacustrine development. Several thousand feet of organic-rich lacustrine clay stones and shales were deposited with interbedded fine-grained sands and silts. The nature of this deposit was probably the result of a humid climate and the lack of external drainage, indicating that the basins were tectonically silled.

The Abu Gabra Formation is estimated to be up to 6,000 ft. (1,829 m) thick. In the northwestern Muglad block, several wells have recovered oil from sands within this sequence. These sands were deposited in

a lacustrine-deltaie environment. The lacustrine clay-stones and shales of this unit are the primary source rock of the interior basins.

Bentiu Formation:

During the late Albian Cenomanian, a predominantly sand sequence (the Bentiu Formation) was deposited. The alluvial and fluvial—floodplain environments expanded, probably due to a change from internal to external drainage. The regional base level, which was created by the earlier rifting and subsidence, no longer existed. These thick sandstone sequences were deposited in braided and meandering streams. This unit, which is up to 5,000 ft. (l,524 m) thick, typically shows good reservoir quality. Sandstones of the Bentiu Formation are the primary reservoirs of the Heglig area.

Darfur Group:

The Senonian period was characterized by a cycle of fine to coarse-grained

deposition. The lower portion of the group, Aradeiba and Zarqa Formations, is characterized by the predominance of claystone, shale, and siltstone.

These initial deposits followed the second rifting phase. The excellent regional correlation of this unit verifies the strong tectonic influence on sedimentation. Floodplain and lacustrine deposits were widespread. The low organic carbon content indicates deposition in shallow and well- oxygenated waters. These units may represent a time when the basins were partially silled. Although this unit offers little source potential to date, it may develop an organic-rich facies in areas not yet drilled. Throughout the basins, the Aradeiba and Zarga formations are an important seal. Interbedded with the floodplain and lacustrine clay stones, shales, and siltstones are several fluvial/deltaic channel sands generally 10-70 ft. (3-21 m) thick. These sands are significant reservoirs in the Unity area. The Cretaceous ended with the deposition of increasingly coarser grained sediments, reflected in the higher.

Amal Formation:

The massive sandstones of the Paleocene, which are up to 2,500 ft. (762 m) thick, are composed dominantly of coarse to medium-grained quartz arenites. This formation represents high energy deposition in a regionally extensive alluvial-plain environment with coalescing braided streams and alluvial fans. These sandstones are potentially excellent reservoirs.

Middle and Upper Kordofan Group:

These sediments represent a coarsening-upward depositional cycle that occurred from the late Eocene to middle Miocene. The lower portion of this cycle, the Nayil and Tendi formations, is characterized by fine-grained sediment related to the final rifting phase. The deposits represent an extensive fluvial-floodplain and lacustrine environment. The lake deposits of this interval appear to have only minor oil source potential; however, they offer excellent potential as a seal overlying the massive sand-stones of the Amal Formation. Upward, this unit is generally characterized by inter-bedded sandstone and claystone with an increasing sand content. The fluvial-floodplain and limited lacustrine environments gave way to the increasing alluvial input reflected in the sand-rich braided stream and fan deposits of the Adok and Zeraf Formations. An exception occurs in the area of the Sudd Swamp where approximately 2,000 ft. (610 m) Of late Tertiary clay stones were deposited.

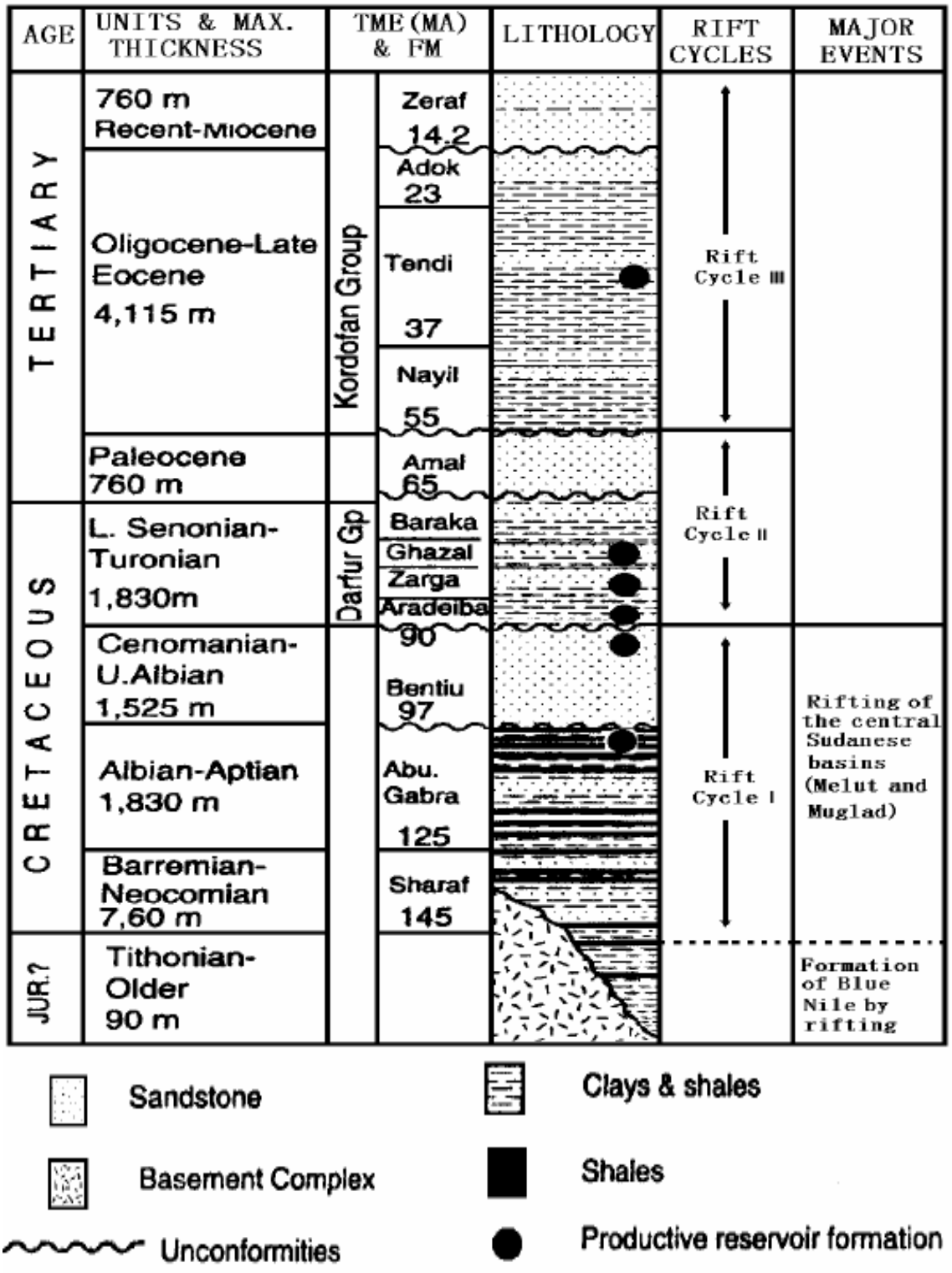

Figure (3): Generalized stratigraphic column for the Muglad Basin showing principal lithologies, maximum formations thickness, producing horizons, and unconformities. cycles rifting

1.4 Problem Statement:

A shale is a fine-grained, indurated sedimentary rock formed by the consolidation of clay or silt. It is characterized by a finely stratified structure (laminae 0.1-0.4 mm thick) and/or fissility approximately parallel to the bedding. It normally contains at least 50% silt with, typically, 35% clay or fine mica and 15% chemical or authigenic minerals. Commonly, clay & shale nomenclature is being used interchangeably among log analysts and petrophysicist.

Shales can cause complications for the petro physicist because they are generally conductive and may therefore mask the high resistance characteristic of hydrocarbons. The clay minerals are ubiquitous in the targeting rocks of oil and gas exploration (Ellis and Singer 2007). They are also subtly variable in chemical composition and can be confused with each other and other silicates.

In reservoir rocks, their presence has an important impact upon reservoir properties such as porosity and permeability and upon those measured physical data that are used to evaluate reservoir quality. Even though they are usually considered to be detrimental to reservoir quality because they can plug pore throats and can be easily compacted, other diagenetic processes may enhance porosity through the forming of secondary porosity through providing porosity by clay dissolution, creating microspores in clays and coating of chlorite on grains to prevent quartz cementation.

Clay crystals attract water that is adsorbed onto the surface, as well as cations (e.g., sodium) that are themselves surrounded by hydration water. It has to be said that core-derived measurements based on crushed samples are probably unrepresentative, since the crushing process will expose many more cation exchange types than will be available in the formation. Moreover, cation exchange capacity per unit pore volume (Q_v) couldn't be related to any log-derived parameter (e.g., porosity, shale volume) with any success.

The recent emerging shale oil and gas exploration requires state-of-art imaging and characterization techniques to study the application of clay minerals in the exploration of this unconventional resource.

Even though there were the numerous sporadic reports about the application of clay minerals in the oil and gas exploration. So far, relatively little work documented the detailed summary of clay minerals from the perspective of oil and gas exploration.

CHAPTER 2

Literature Review:

The oil prone of the Niger Delta, most of its reservoir hydrocarbons produced by using detailed geological, petro physical knowledge and data are needed to guide the placement of the well paths. Shale correction leads to a significant change in petro physical parameters. The Simandoux and Indonesian models are both suitable for water saturation, and hydrocarbon saturation analysis in shaly sands. The various lithologies through the log profile can be deduced using the gamma ray log. Any deflection that touches the shale base line is that of a clean shale formation and any deflection on the sand line, is that of a clean sand formation. Intermediary deflections are considered as deflections of complex lithology formations. It can illustrate the changes in the values of the petro physical parameters, shale corrections are neccessary, and the variation of these parameters with changes in the shale volume. The interpretation of shaly-sands log data can be of a challenge. There are more than 30 shaly sand interpretation models, which have been developed in the last 50 years. Interpretation difficulties arise whenever the portions of clay minerals in a shaly-sand formation are high. An increase in effective porosity (uncorrected) can be caused with the increase of shale volume. This increase in porosity with increase in shale volume, can be accounted for by the fact that shales has its own porosity, and add to the sand porosity in the reservoir. (K., et al., 2019)

At the Niger Delta a study was conducted which shows that the combination method was the most reliable for estimating shale volume which fall within the acceptable range. The challenge that is posed in this case is how net sand is defined and what constitutes valid criteria for differentiating net reservoir from non-reservoir intervals. A comparative analysis of all the methods in estimating V_{sh} in shaly sand units, taking into consideration the strengths and limitations of the logs is therefore necessary. The lithology logs (SP and GR) should be used together only because they compensate for each other, if a deflection does not show the same pattern on both logs, then there must have been a radioactive effect or lithological change. The GR direct linear measurement overestimates the volume of shale in radioactive sand units, as discovered from comparison with established volume of shale cut-offs from previous studies, used to classify the volume of shale values as acceptable, unacceptable and fair. The volume of

shale estimated from other methods, can show a reduction in the shale volume values relative to the linear method. (Fadiya, Alao, O. A, & Adetuwo, A. M, 2018)

Fluid saturation is the fraction of the pore volume of the reservoir rock that is filled with liquid (water, oil) and gas or single phase. The assessment of hydrocarbon saturation of thick shaly sand reservoir conducted at Bhuban formation of the onshore fields of Bengal Basin, Bangladesh. Lithology can be identified from natural gamma ray log where hydrocarbon bearing zone is detected by resistivity and lithology log including cross checking of porosity logs. From gamma ray method shale volume could be estimated, while effective porosity could be found from neutron-density combination formula with clay correction. Inverse Archie's model is used for the estimation of formation resistivity. The Simandoux, Indonesia, Fertl and Hammack models have been used for water saturation assessment. The lithology in the Bhuban formation is laminated shale and several sand zones present in the well. Shale, shaly sand and sand zones have been identified with respect to Gamma Ray where high and low GR response indicates the shale or clay zone and clean sand zone, respectively. By the use of Caliper log, comparing with Bit size of drill hole permeable zones could be detected. Hydrocarbon bearing zone is also detected from lithology logs and resistivity with indicating cross-over of Neutron-Density logs. It indicates that the shale volume is changed due to the changes of radioactive properties with respect to depth. (Tamim & Mohamed Miah, 2015)

Shaly sand interpretation is still sprouting with numerous researchers conducting investigations of the clay minerals effect on rock conductivity through the theoretical and experimental approach. In Palouge-Fal oilfield, Melut basin, old South Sudan a model is proposed based on experimental work on homogenous mixtures of sand and montmorillonite. Poupon and Leveaux developed a model based on field data from Indonesian where the reservoir rock has fresh formation water and high degree of shaliness. The model is known as "Indonesia formula". Hill and Milburn indicated a non-linear logarithmic relationship between formation resistivity and formation water resistivity using large amount of water saturated shaly sand core samples. They also demonstrated that cation exchange capacity (CEC) can be used as an effective shaliness indicator. Waxman-Smits proposed a shaly sand model based on the data from Hill and Milburn

in addition to data from their own measurements. The conductivity of water saturated shaly sand is directly related to the shaliness factor, conductivity of formation water, and porosity. The performance of various shaly sand saturation equations must be compared to the water saturation calculated from drainage capillary pressure. The wireline logging, mud logging, well testing, and core data should be carefully evaluated during the processing of the data in order to get a good quality data. Almost all kinds of petro physical parameters should be used for log interpretation and accomplished with processing and interpretation, including interpretation of the results, tabling, plotting and cross-plots making for data quality control. Consequently, the methods and techniques in the shaly sand models can be used to improve petro physical evaluation of shaly sand reservoirs. A new method was used to identify reservoir quality by using spectral gamma ray. Also this method was used to investigate the production by swabbing and low flow rate despite the oil produced from such zones sometimes have high API value. All of the evaluated shaly sand equations produced acceptable saturation results for the shaly sand reservoirs as long as suitable shale parameters are selected. The success in using a given equation depends mainly on the skill of the log analyst in integrating all available information into his or her analysis as well as familiarity with the equation(s) s/he is using. Open hole logging data are competent for oil/water zone identification. (Hussein & Ahmed, 2012)

CHAPTER 3

Methodology:

The evaluation of the formation was carried out using a composite of well logs mainly Gamma ray, Neutron, Density, Resistivity and Sonic logs, supported with core laboratory measurements. The enterprise includes lithology, identifying the permeable hydrocarbon bearing zones and quantification evaluation of shale volume, formation porosity, saturation, and permeability computation from logs.

3.1 Lithology identification:

The lithology identification penetrated by any well involves a combination of different logging curves, the logs used to identify the lithology are the Gamma ray, Neutron and density logs. The Gamma-ray and neutron-density cross plot were examined for lithological discrimination. The Gamma ray which measures the natural radioactivity reflects clay contents in the formation while the neutron-density cross plot is used to differentiate the type of lithology. The resistivity log and Gamma ray logs are utilized to discriminate the sandstone and shale formations. Based on the log response of the whole intervals of the four wells (Jake-2, Jake-28, Jake-34 and Jake-37), each well was divided into different zones. The identification of different zones is supported by relatively low and high gamma ray readings (track 1) which and the green vertical line (Shale) respectively as shown in figure (3), the resistivity readings and the crossover between neutron and density curves suggests the changes of lithology and fluid types in the formation.

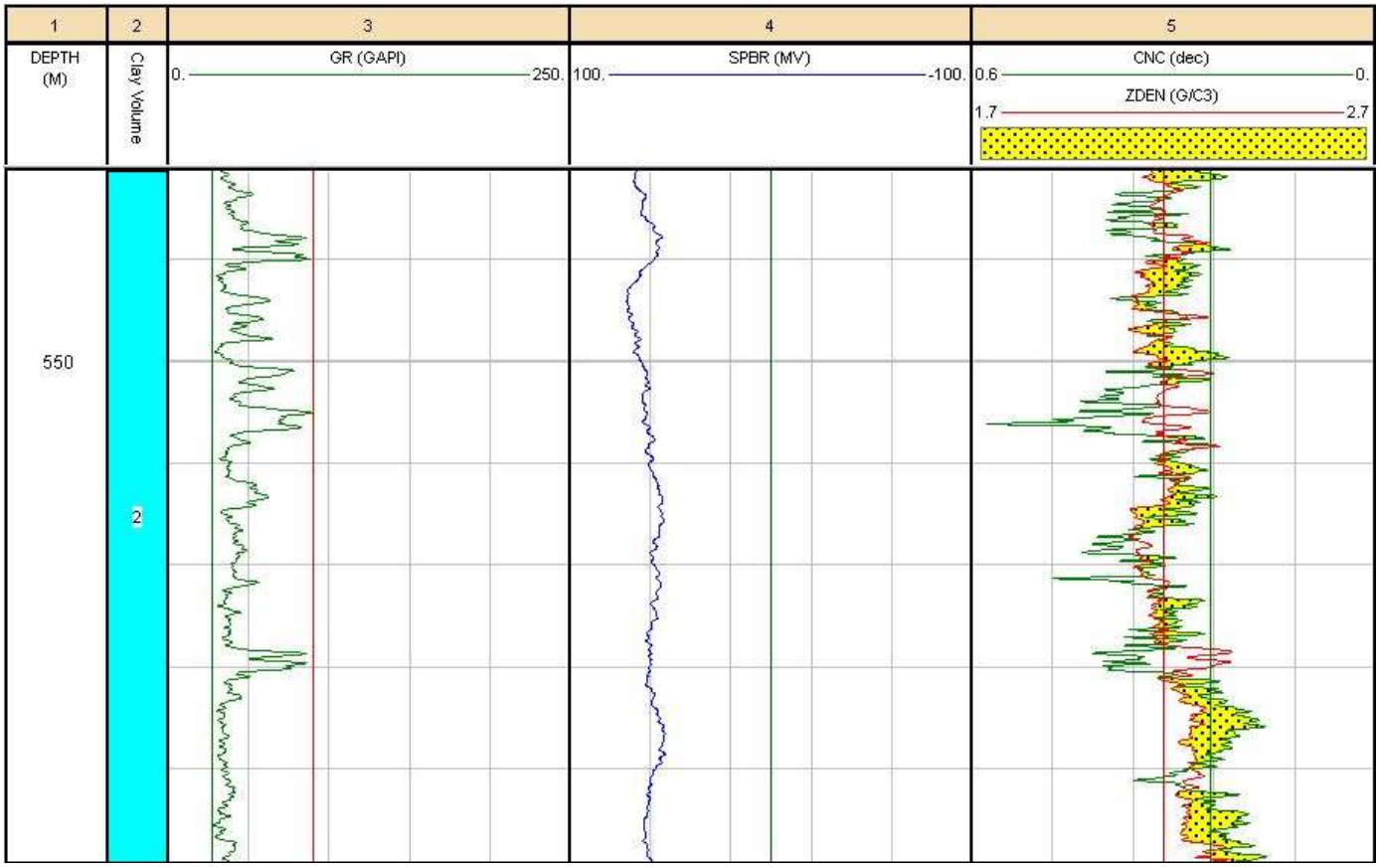

Figure (4): Identifying Lithology

3.2 Shale Volume Estimation:

The shale volume (V_{sh}) was computed from the gamma ray plot, Neutron density cross plot and using the resistivity logs. Another way of calculating the shale volume is by using the equation below which utilizes the values of Gamma Ray (GR):

$$V_{sh}Larinov\ Tertiary\ Rocks = 0.0832(2^{3.71*I_{GR}} - 1) \quad \textbf{Equation (3.2.3)}$$

Where;

V_{sh}= shale volume

I_{GR}= Gamma ray index

The gamma ray index (IGR) is estimated from the following relationship:

$$I_{GR} = \frac{GR_{log} - GR_{min}}{GR_{max} - GR_{min}}$$ **Equation (3.2.3)**

where,

GR **log**= measured GR from log

GR **min**= GR reading in the zone of interest

GR **max**= maximum GR reading in the zone of interest

Shale Volume for neutron-density combination log method utilized the Crain's neutron-density chart:

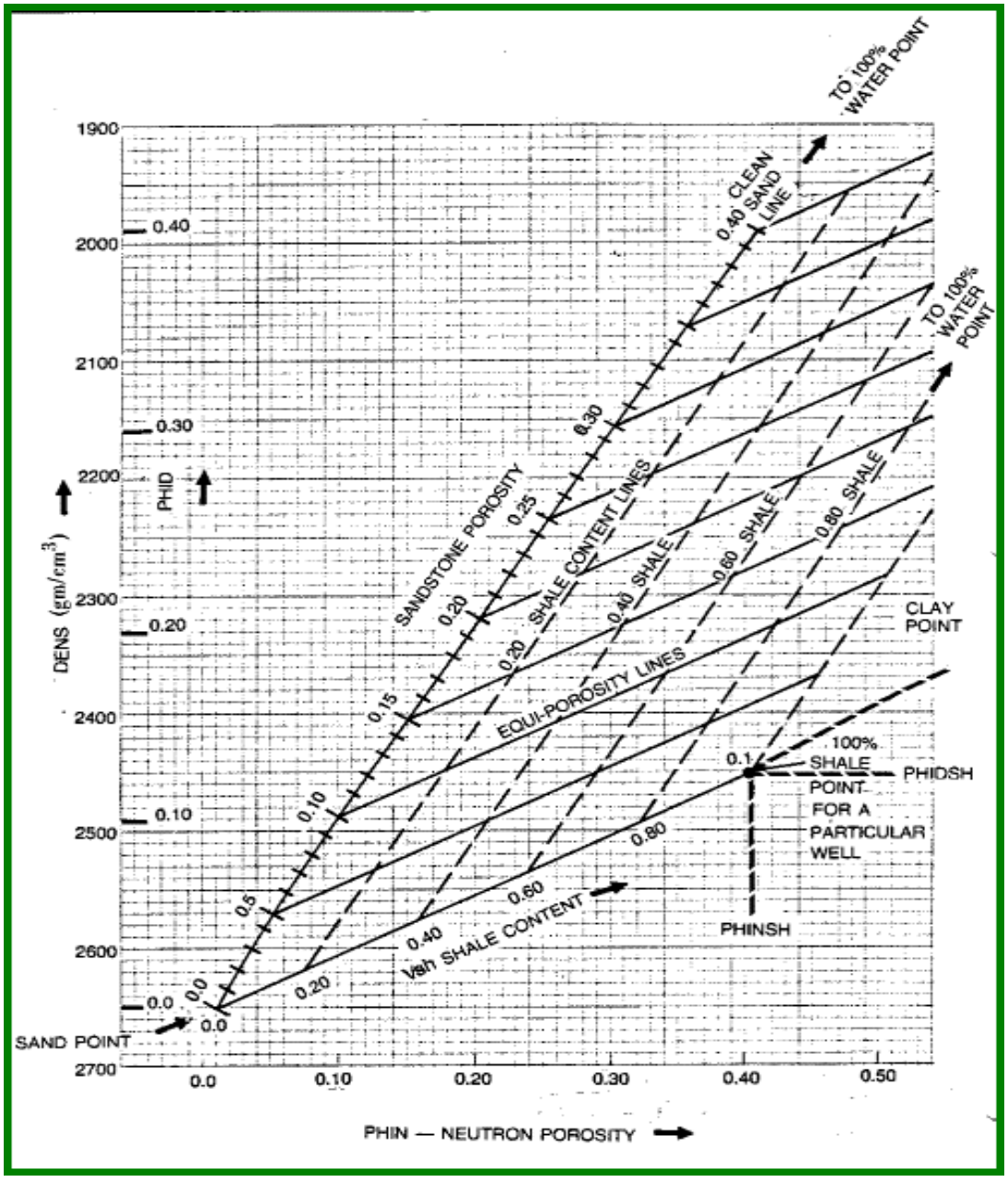

Figure (5): Neutron-Density Cross Plot

3.3 Temperature Gradient:

The temperature gradient is calculated by inputting the surface temperature and the bottom hole temperature fixed points that were obtained from the provided data of the four wells (Jake-2, Jake-28, Jake-34 and Jake-37) and the program had extrapolated between the fixed points. The temperature gradient is entered in degree per meter, depending on the unit of the well. A reference depth and temperature is also needed to be entered to give starting point for the temperature curve. The output curves are important and used in the interpretation models to make the correct temperature gradient.

$$\textbf{Temperature Gradient} = \frac{BHT - T_o}{TD} \qquad \textbf{Equation (3.3.4)}$$

Where;

BHT = Bore hole temperature

T_o = Surface Temperature

TD = Total Depth

3.4 Porosity Determination:

Porosity is the fraction of voids of the total volume of the rock. There are many equations often used to estimate either effective or total porosity from well logs. In this study, the method being used is the N-D method (combined neutron-density porosity logs as provided by Interactive Petrophysics software). Porosity can be determined from direct measurements (neutron) or can be calculated from various logs e.g. neutron and density, sonic, and density. It can also be obtained from combination logs. neutron and density logs.

3.4.1 Total porosity:

Total porosity is defined as the ratio of the entire pore space in a rock to its bulk volume. The Density log was used to calculate porosity. Density-derived porosity (porosity from density log), is computed using the equation:

$$\boldsymbol{\varphi_T = \left(\frac{\varphi_N^2 + \varphi_D^2}{2}\right)^{\frac{1}{2}}} \qquad \textbf{Equation (3.4.5)}$$

ϕ_N= Porosity from Neutron log.

ϕ_D = Porosity from Density log.

3.4.2 Effective porosity:

Effective porosity is the total porosity less the fraction of the pore space occupied by shale or clay. In very clean sands, total porosity is equal to effective porosity The neutron-density combination is still often the most reliable technique to estimate formation porosity from well logs. However, inaccurate characterization of matrix yields less accurate porosity and saturation estimates especially in complex lithology (thin laminated layers), the effects of shale on density tool greatly depend on the density and type of clay minerals. The formula used to compute the effective porosity is shown below:

$$\varphi_e = \left|\frac{\varphi_D(\varphi_N)_{sh} - \varphi_N(\varphi_D)_{sh}}{(\varphi_D)_{sh} + (\varphi_N)_{sh}}\right| \qquad \textbf{Equation (3.5.6)}$$

Where;

$Ø_D$ = Density Porosity

$Ø_{Dsh}$ = Density Porosity in shale formations

Øe = Effective Porosity

$Ø_N$ = Neutron Porosity

$Ø_{Nsh}$ = Neutron Porosity in shale formations

3.5 Permeability:

Rock permeability is one important flow parameter associated with subsurface production and injection; it is an intrinsic characteristics of the materials that determines how easily the fluids can pass through it. Estimation of permeability from well logs has a particular advantage of the economy due to their continuity measurements. In fact, permeability is a complex parameter to determine because it is affected by many factors such as size of the matrix grain, type, amount and distribution of clay minerals, porosity, and many other factors.

In normal reservoir, permeability can be accurately estimated from porosity because of good relationship that exists between porosity and permeability of these reservoirs. Therefore, permeability in this study was obtained from inserting the equation formed from the porosity – permeability cross-plot into the Interactive Petrophysics software.

3.6 Porosity-Permeability relationship:

The cross plot between the core porosity and core permeability may vary and an equation could be formed from this relationship, the trend may reflect the deposition sequence within the basin. Using a formula where permeability is a function of porosity may lead to inaccurate results, because shale formations that have high porosities will result in high calculated permeability when inputting the equation into the software. Correlation between calculated permeability and core permeability is needed to ensure the validity of the equation formed from the permeability and porosity relationship.

3.7 Determination of Formation Water Resistivity (R_W):

Formation water is the water uncontaminated with drilling mud. The resistivity of the formation water (R_w) is an important interpretation parameter since it is required for the calculation of saturations. There are several sources for formation water resistivity information. In all cases, a good value of R_w can be easily found from the water sample measurement. Water resistivity in this study was obtained from total porosity and deep laterolog resistivity Pickett cross plot. A shaliness discriminator of 0.40 was used in all zones.

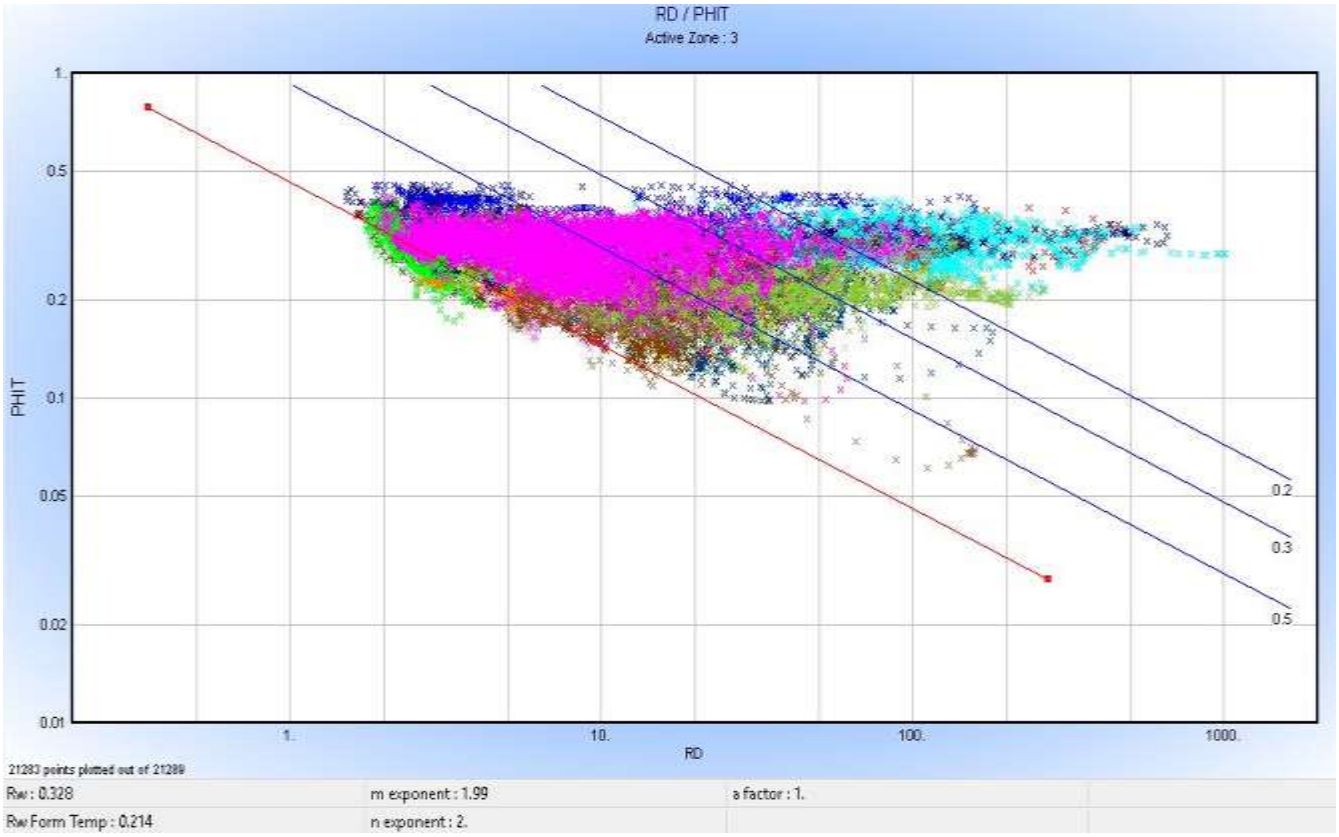

Figure (6): Picket Cross plot

3.8 Water Saturation Calculation (S_w):

Water saturation is the fraction fluid of the pore volume occupied by water. The ultimate of any petro physical analysis and evaluation is to compute water saturation in the reservoir. Because the economic production decisions of hydrocarbon from a potential reservoir mainly depend on

rock water saturation. Furthermore, it is an important component in determining the hydrocarbon saturation.

Determination of water saturation (S_w) from well logs is very challenging because there many equations available to deliver it. Unfortunately, there is no unique equation for shaly models accurately estimate it except for the clean reservoirs in which Archie`s equation have proved successfully. In shaly-sand reservoir, each equation tends to produce different water saturation values due to varying amount, distribution, and the associated bound water of shale or clays. For this study, the reservoir is evaluated using three different saturation equations which includes Archie, Indonesian and Simandoux. It is worth emphasizing that each of these equations is differently affected by shale as explained above in additional to model parameters. In petro physical formation evaluation, water saturation can be calculated from different saturation models depending on whether the reservoir is clean or shaly.

Archie Model:

The log interpretation for evaluation of hydrocarbon saturated permeable formation is based on Archie's equation, which relates the water saturation to formation water resistivity, porosity and resistivity of saturated formation, this relationship is given by the following Archie's Equation:

$$S_W^n = \frac{a * R_W}{\varphi^m * R_t} \qquad \textbf{Equation (3.9.7)}$$

Indonesian Model:

The model is used for calculating effective water saturation in shaly sand formations and is independent of the shale distribution in the reservoir. The relationship between the formation resistivity and the formation parameters affecting it (includes R_w, R_{sh}, S_w, and V_{sh}) was proposed and is given by the following equation:

$$\frac{1}{\sqrt{R_t}} = \left(\frac{V_{sh}^{\left(1-\frac{V_{sh}}{2}\right)}}{\sqrt{R_{sh}}} + \frac{\varphi^{\frac{m}{2}}}{\sqrt{aR_w}} \right) S_{we}^{\frac{n}{2}} \qquad \textbf{Equation (3.9.8)}$$

Simandoux Equation:

The experiment studies by the Simandoux on artificial homogeneous mixtures of sand and clay (montmorillonite) have suggested that the conductivity (resistivity) can be expressed by the following relationship:

$$\frac{1}{R_t} = \frac{\varphi^m}{aR_w} S_W^n + \frac{V_{sh}}{R_{sh}}$$ **Equation (3.9.9)**

where,

a = tortuosity

m = cementation factor

n = saturation exponent

R_w = formation water resistivity

R_{sh} = shale resistivity

R_t = formation resistivity

S_w = water saturation

ϕ = formation porosity

3.9 Net Pay:

The net pay is the thickness that contains economically productive interval. It was determined by applying cut-offs to rock properties. Water saturation cut-offs value of 50% was used. The net pay was considered to contain hydrocarbon if the (Sw<=50%) within the reservoir.

3.10 Hydrocarbon Movability Index (Sw/Sx)

This is the fraction of the uninvaded water saturation (Sw) and the flushed zone water saturation (Sxo). The ratio of the Sw/Sxo has an important indication on the movability of hydrocarbon. For Sw/Sxo greater or equivalent to 1 indicating that the hydrocarbon is immoveable. For values less than 0.7 indicating that the hydrocarbon is moveable.

$$S_{xo}^{n} = \frac{a * R_{mf}}{\varphi^{m} * R_{xo}} \qquad \textbf{Equation (3.10.10)}$$

Where;

S_{xo} = Flushed zone water saturation

R_{mf} = Mud filtrate Resistivity

3.11 Cut-Off:

There have been many different approaches to quantifying cutoffs, with no single method emerging as the definitive basis for delineating net pay. Yet each of these approaches yields a different reservoir model, so it is imperative that cutoffs be fit for purpose, they are compatible with the reservoir mechanism and with a systematic methodology for the evaluation of hydrocarbons in place and the estimation of ultimate hydrocarbon recovery. These different requirements are accommodated by basing the quantification of cutoffs on reservoir-specific criteria that govern the storage and flow of hydrocarbons. In doing so, particular attention is paid to the relationships between the identification of cutoffs and key elements of the contemporary systemic practice of integrated reservoir studies. The outcome is a structured approach to the use of cutoffs in the estimation of ultimate hydrocarbon recovery. The principal benefits of a properly conditioned set of petro physical cutoffs are a more exact characterization of the reservoir with a better synergy between the static and dynamic reservoir models. The cutoff was computed by interpreting the data using the Interactive Petro physics program.

CHAPTER 4

Results and Discussion:

In this study area, the sand units are considered as the reservoir units because shale is not porous and permeable enough to host, retain and release fluid. In the formation units described, the resistivity of hydrocarbon is higher than that of the formation water and hydrocarbon sand units were inferred from high resistivity values observed so the reservoir fluids (hydrocarbon and water) were distinguished by using the resistivity logs **figure (7).** The lithology logs (SP and GR) were used together only because they compensate for each other, if a deflection does not show the same pattern on both logs, then we can infer that there must have been a radioactive effect or lithological change**.**

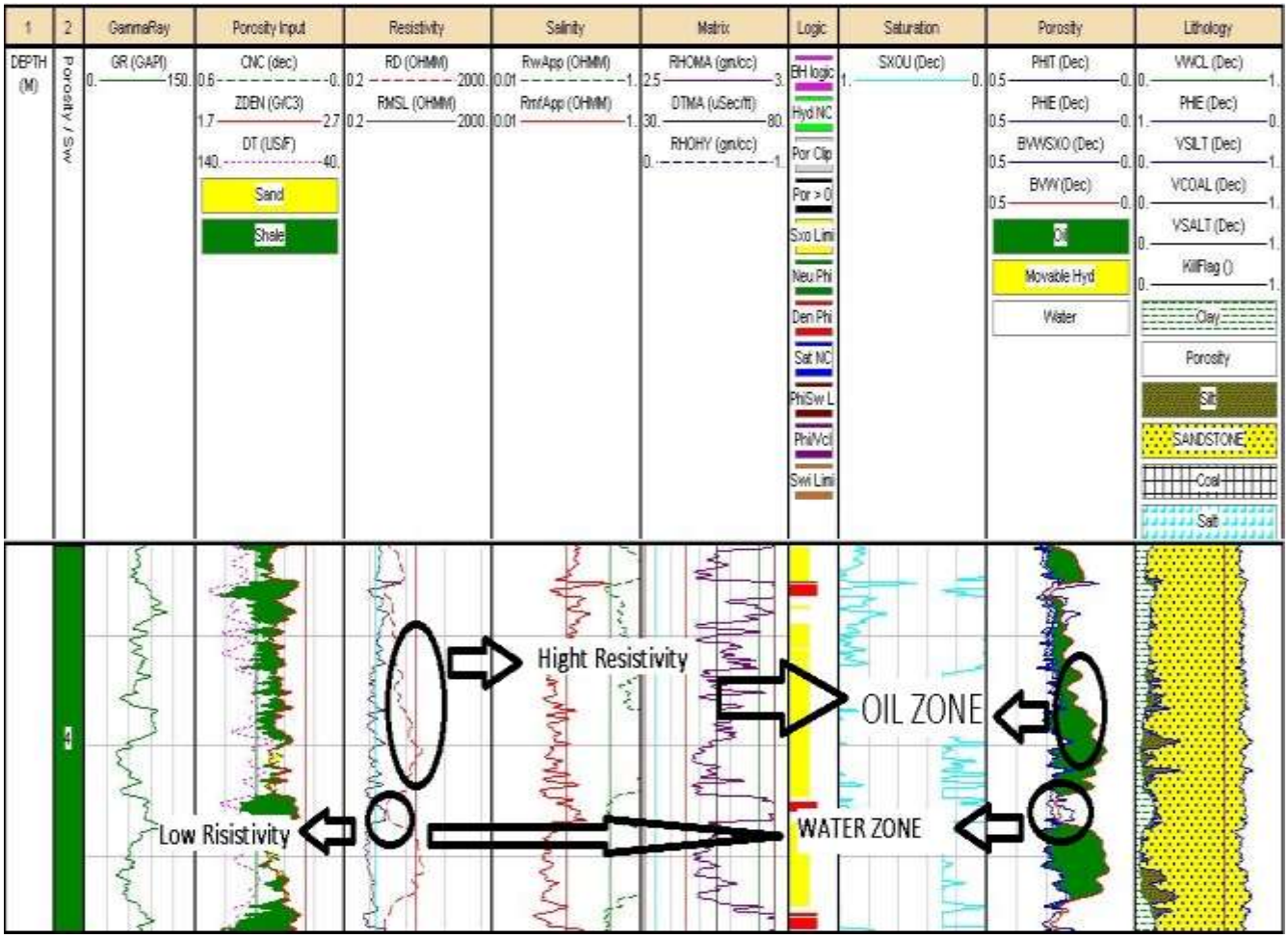

Figure (7): Fluid Identification

4.1 Quantitative Evaluation:

At the depth of 1303m in Aradeiba formation, the zone is marked by high gamma ray (track 1) and a large separation between neutron and density curves (track 2) with low resistivity readings (track 3) as shown in **figure (9)**. Based on the observation made, this zone is suggested being a mainly shale zone with low potential to be a commercially hydrocarbon zone.

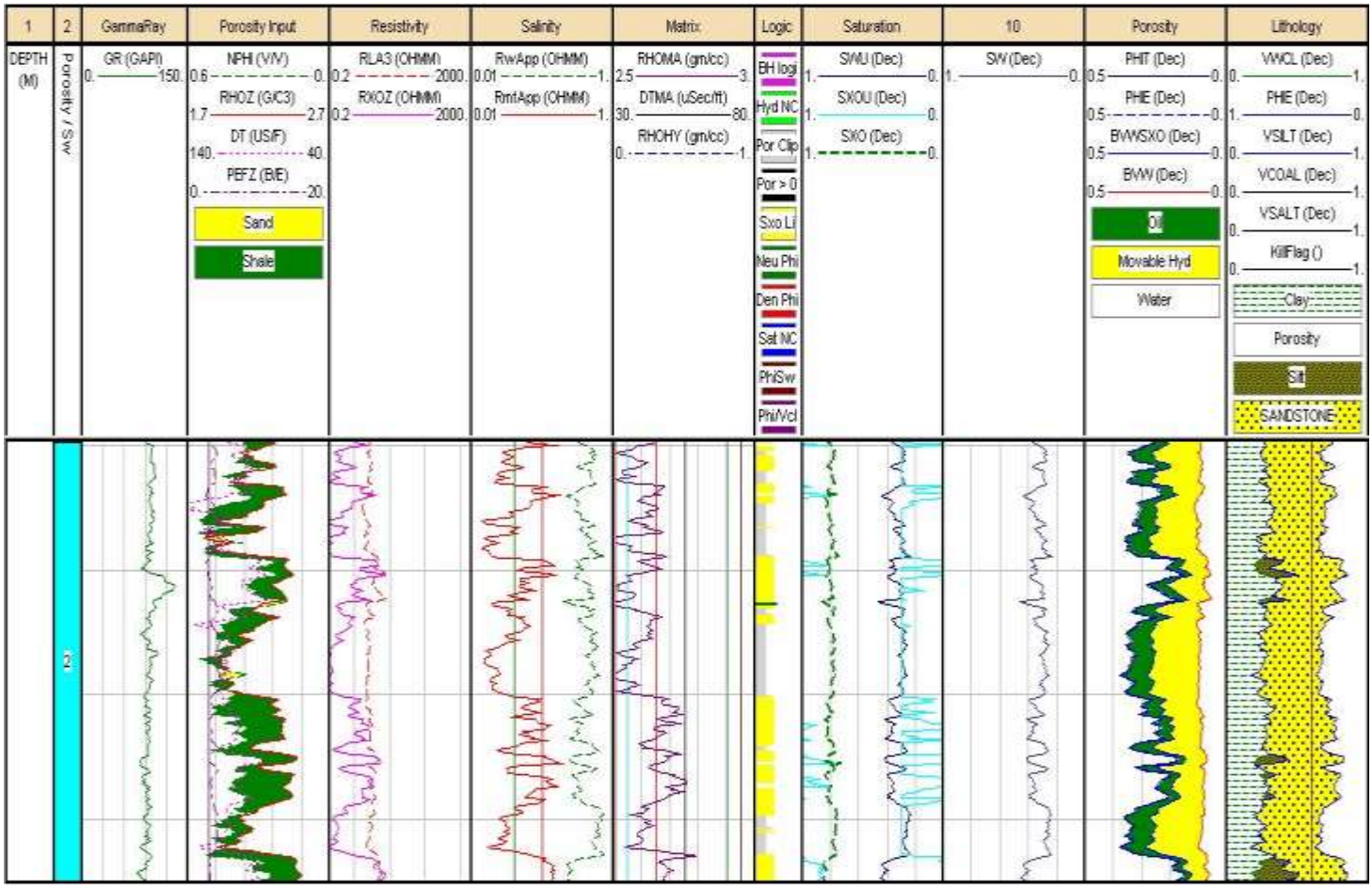

Figure (8): Shaly sand identification

In **figure (9)** at the depth of 1475m in Bentiu formation, the zone is marked by the relatively low gamma ray, high resistivity readings and low density with high neutron readings. Combining these observations, the zone is confirmed to be an almost clean sandstone with very minor amount of shale interval.

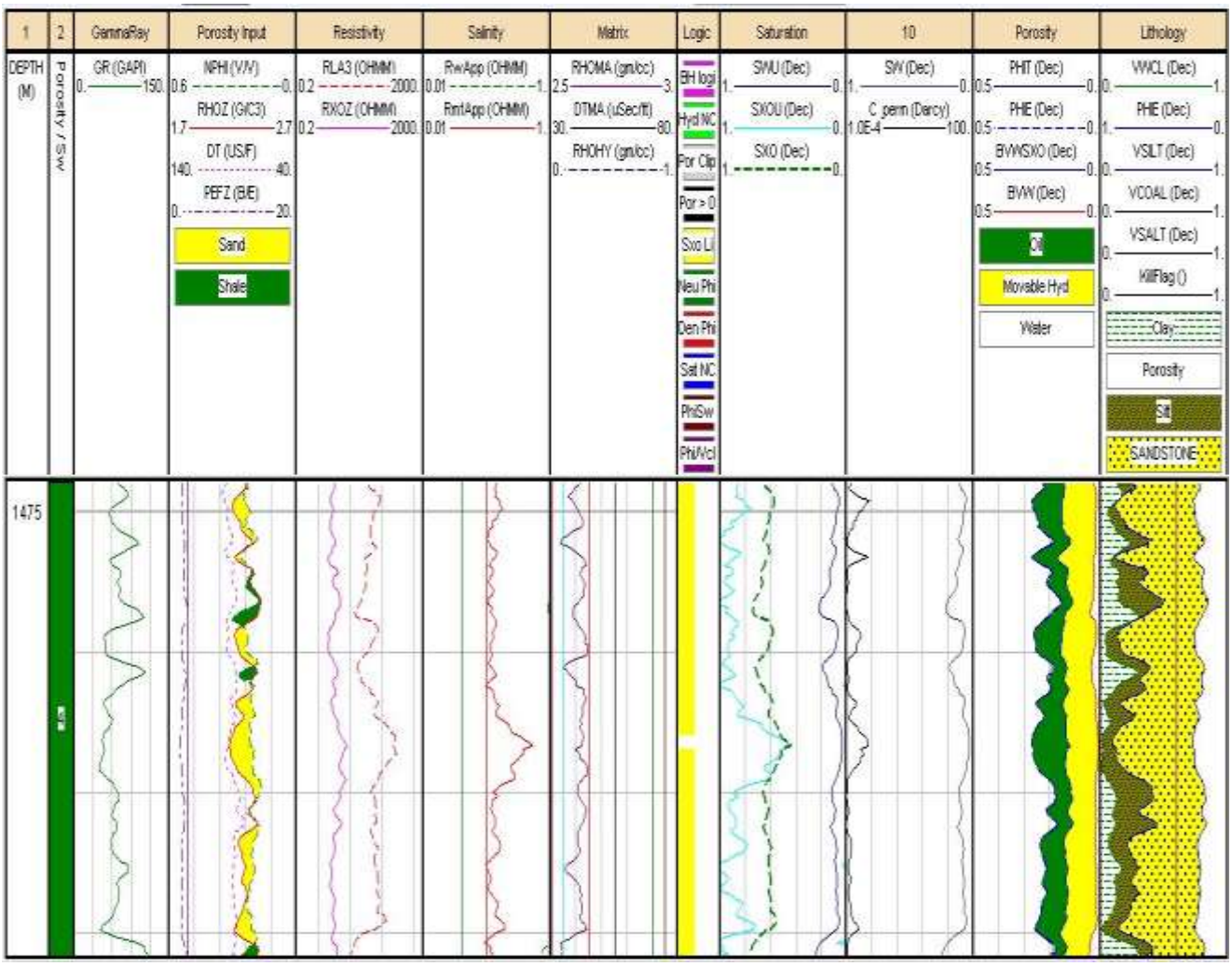

Figure (9): Clean sand determination

In Bentiu formation at the depth of 1675m, the identification of the zone in **figure (10)** is supported by relatively low gamma ray reading, the crossover between neutron and density curves which suggests for the change of lithology and fluid types in the formation. From this observations, this zone is interpreted as being the shaly sand zone.

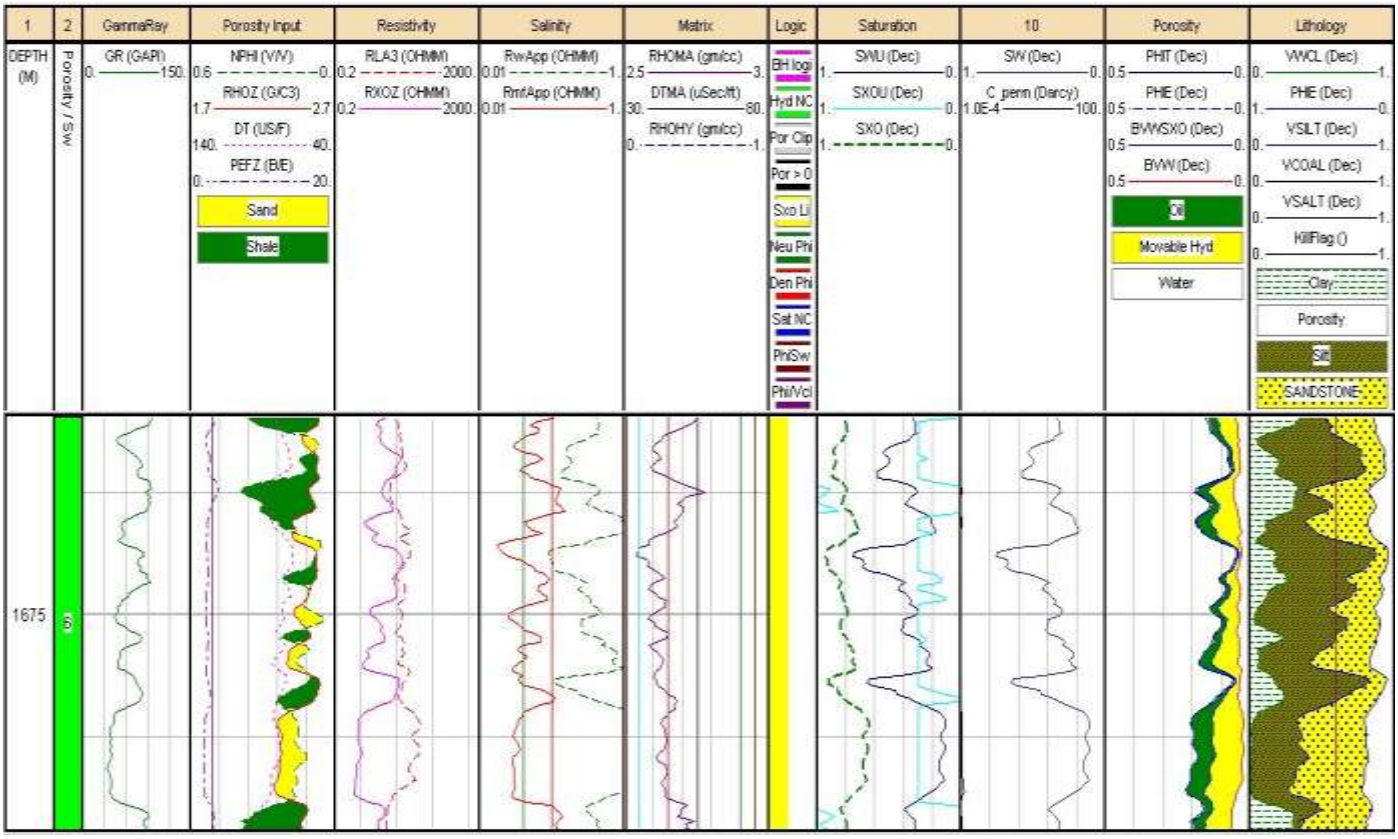

Figure (10): Shale zone

4.2 Formation Porosity (Ø):

Figure (11) compares the log-derived porosity with the core porosity. The underestimation of porosity neutron-density technique is that this method relies on the neutron and density logs to deliver the effective porosity. Light hydrocarbons or gas-bearing formation makes a difference in neutron porosity and density tools response. Shaliness in the formation may again influence the effective porosity from neutron and density logs. The nature and their associated bound water of

the clay minerals have an influence on neutron tools response by increasing the apparent neutron porosity. But, their effect depends on clay mineral type available in the formation.

In oil zone or water-bearing zone, the underestimation of the effective porosity by the neutron-density technique can be checked against core-derived porosity when plotted in the same log scale. The average porosity from the neutron-density (27.3) %.

The porosity derived from core data is showing very good matching with that log porosity as can be shown from **figure (11).**

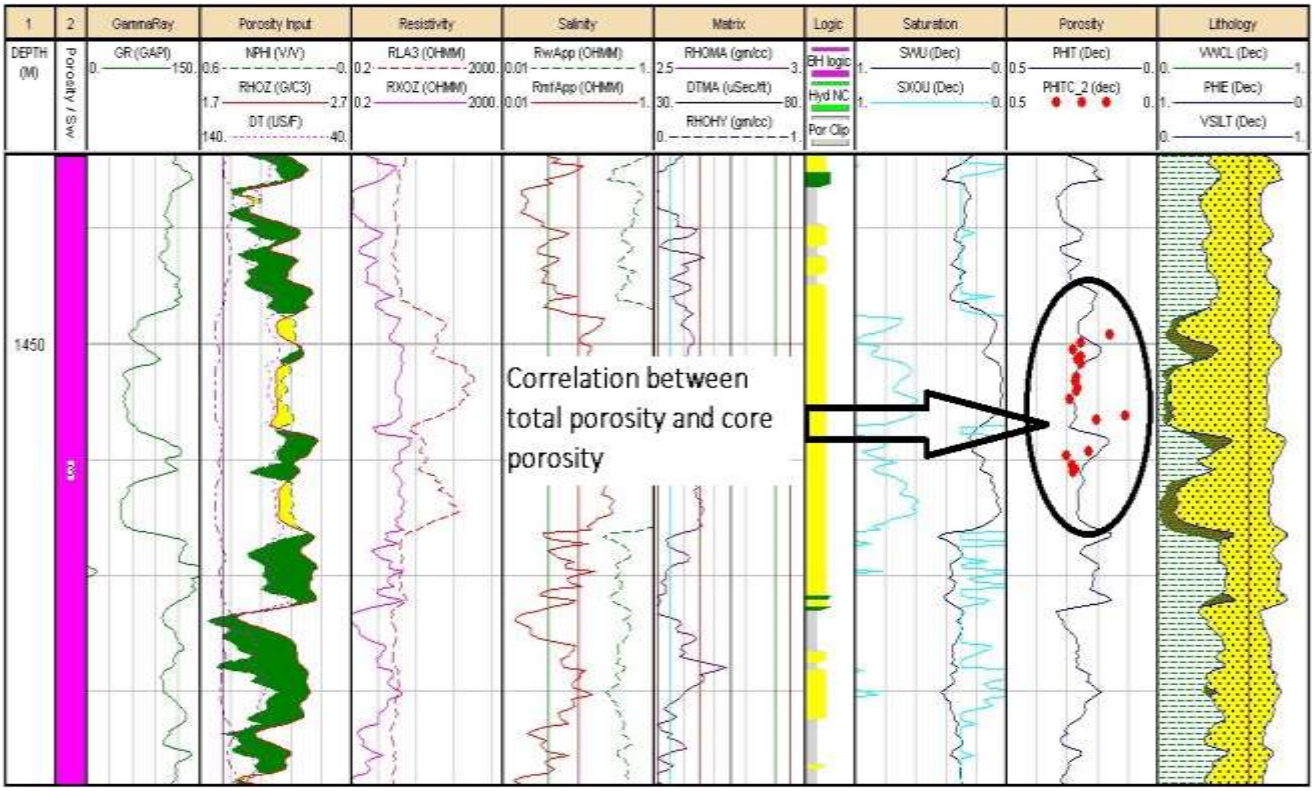

Figure (11): Correlation of total porosity with core porosity

4.3 Permeability:

The formation permeability was calculated by cross plotting the porosity and permeability values from the core data of Jake-South S2. An exponential equation between the porosity and permeability was inferred using excel spread sheet and input into the Interactive Petro physics

software as a result a curve indicating the permeability values along the different zones was obtained.

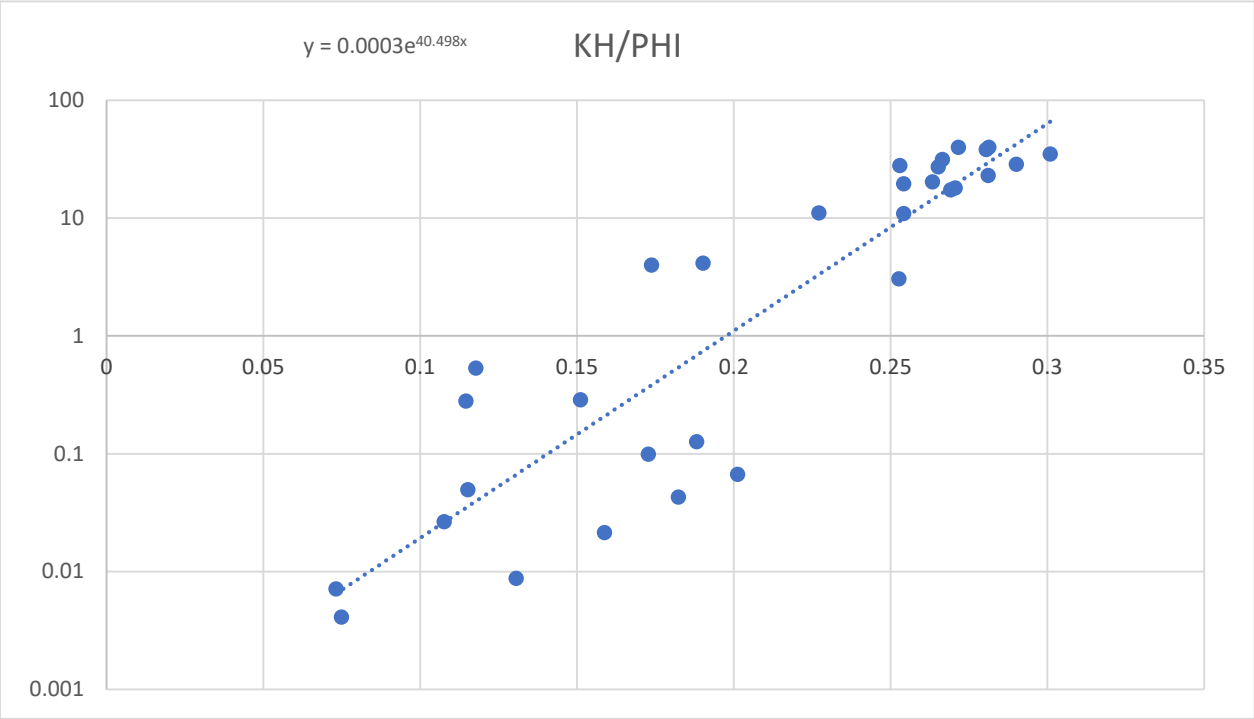

Figure (12): Permeability and porosity cross-plot

$$y = 0.0003e^{40.498x}$$ **Equation (4.3.11)**

Where;

y= Calculated Permeability

x= Total Porosity

So far, shale is built of micro and Nano sized space pores which can have high porosities and the permeability calculated is a function of porosity, this resulted in high permeability values across shale formations as shown in **figure (12).**

Due to the limited core data available calibration is made using the same permeability values to the different other wells as shown in **figure (14).**

4.4 Correlation between calculated permeability and core permeability:

In **figure (13)** the values of the calculated permeability and the core permeability are almost close which indicates that the formula conducted from the permeability and porosity cross – plot is useful and suitable for correlation and can be used in calibration for other wells.

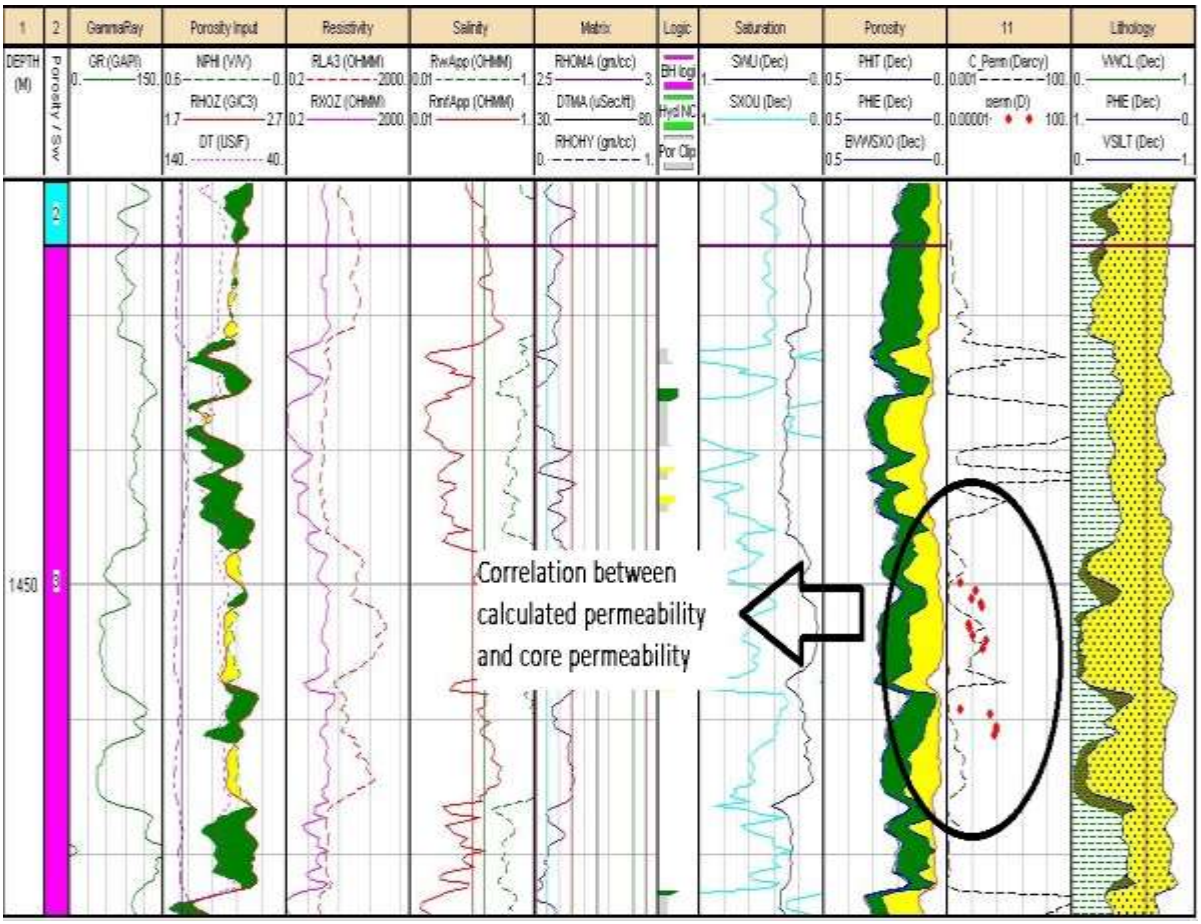

Figure (13): Correlation between calculated permeability and core permeability

4.5 Water saturation (S_w):

In shaly-sand reservoir, the Archie model often overestimates the water saturation as explained in literature review. The apparent differences in the estimated average water saturation values from all shaly sand equations can be expected to vary when the amount of shale or clay in

potential zone varies. Not only by varying the amount of shale but also the way the shale is distributed in the potential reservoir.

Since the entire reservoir is observed to be a mixture of clean sand and shale formations **figure (13)**. The average water saturation is calculated using all mentioned saturation models. It is observed that one may attempt to even apply any model (Archie or shaly sand models) in formation with a minimal or null shale contents. However, in a low shaliness reservoir the Archie model still remains the best technique due to few parameters that needs to be computed before applying the model. The shaly sand saturation models involve a clean term (Archie term) and a shale term, then it is now clear that, the shale term drops to zero or insignificant value when the amount of shale vanishes and all shaly saturation equations revert to clean model (Archie model).

4.6 Correlations of water and oil saturations:

Archie's method:

Tables (2)(3) summarizes results from Archie model. The model estimated higher water saturation (S_w) relatively to shaly sand models. The reason is being the shale or clays effects. Shale or clays have an important impact on most logging tools such as porosity and resistivity logs. Since S_w is a function of formation resistivity (R_t), porosity ($\emptyset$), and water formation resistivity (R_w). The presence of shale or clays lowers (suppress) the formation resistivity by the excess conductivity of shale and clay minerals. Archie assumed that only fluid in the pores is conductive which is opposite to shale matrix being conductive. Suppression of formation resistivity by the shale effects causes an error that is directly translated to S_w value. This is the source of an overestimation of S_w value from the model.

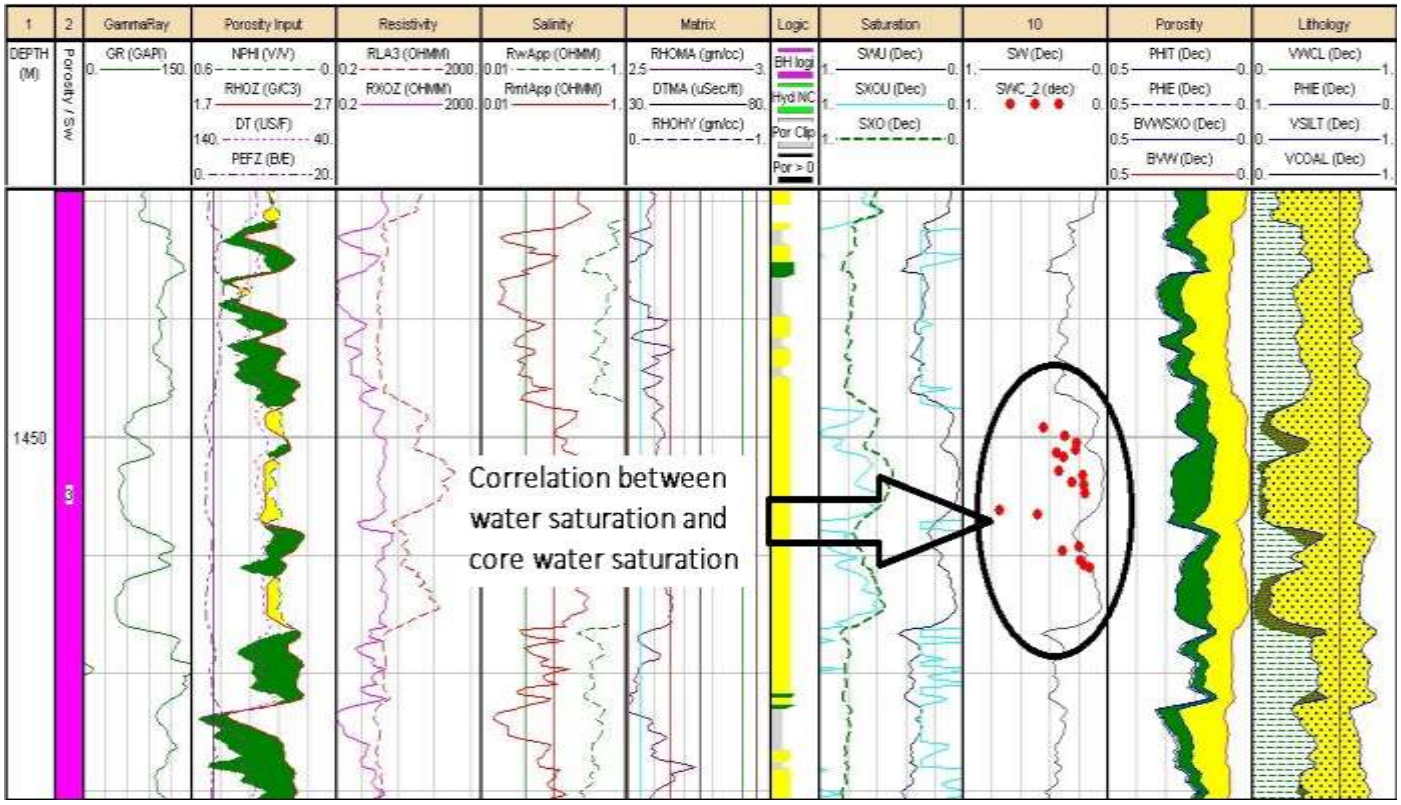

Figure (14): Correlation between water saturations with core water saturations values using Archie model

Reservoir Summary:

Zn	Zone Name	Top	Bottom	Gross	Net	N/G	Av Phi	Av Sw	Av Vcl	Av perm	Av sxo	Phi*H	PhiSo*H	Vcl*H	perm*H	sxo*H
#									Ari	Ari	Ari					
1		172.97	1301.64	1128.67	1115.79	0.989	0.274	0.272	0.175	150.935	0.759	305.89	222.56	194.81	168411	847.37
2		1301.65	1437.44	135.79	135.79	1	0.275	0.284	0.255	248.1		37.3	26.71	34.58	19026253	
3		1437.44	1473.56	36.12	36.12	1	0.249	0.234	0.272	26.795	0.729	8.98	6.88	9.81	967.8	26.32
4		1473.56	1563.32	89.76	87.33	0.973	0.198	0.175	0.194	6.527	0.697	17.3	14.28	16.97	569.99	60.9
5		1563.32	1575.82	12.5	12.5	1	0.189	0.323	0.335	2.018	0.793	2.37	1.6	4.18	25.22	9.91
6		1575.82	1761.9	186.08	147.9	0.795	0.171	0.206	0.131	1.108	0.728	25.25	20.06	19.44	163.91	107.61
7		1761.9	1839.93	78.03	64.24	0.823	0.159	0.157	0.1	0.378	0.69	10.2	8.59	6.39	24.27	44.33
8		1839.93	1854.25	14.33	12.19	0.851	0.139	0.412	0.349	0.218	0.838	1.7	1	4.26	2.66	10.22
9		1854.25	1887.17	32.92	25.83	0.785	0.168	0.127	0.096	0.481	0.659	4.35	3.8	2.49	12.41	17.03
	All Zones	172.97	1887.17	1714.19	1637.68	0.955	0.252	0.261	0.179	126.67	0.748	413.34	305.47	292.94	19026255	1123.68

Table (1): Reservoir summary from the cutoff for Archie model

Pay Summary:

Zn	Zone Name	Top	Bottom	Gross	Net	N/G	Av Phi	Av Sw	Av Vcl	Av perm	Av sxo	Phi*H	PhiSo*H	Vcl*H	perm*H	sxo*H
#									Ari	Ari	Ari					
1		172.97	1301.64	1128.67	1097.8	0.973	0.275	0.264	0.171	153.083	0.756	301.63	222.13	188.2	168055.5	829.88
2		1301.65	1437.44	135.79	135.33	0.997	0.275	0.284	0.255	24809857		37.24	26.68	34.46	19026253	
3		1437.44	1473.56	36.12	36.12	1	0.249	0.234	0.272	26.795	0.729	8.98	6.88	9.81	967.8	26.32
4		1473.56	1563.32	89.76	86.87	0.968	0.198	0.173	0.194	6.56	0.696	17.23	14.25	16.84	569.82	60.48
5		1563.32	1575.82	12.5	12.5	1	0.189	0.323	0.335	2.018	0.793	2.37	1.6	4.18	25.22	9.91
6		1575.82	1761.9	186.08	147.75	0.794	0.171	0.205	0.131	1.109	0.727	25.23	20.05	19.41	163.9	107.47
7		1761.9	1839.93	78.03	64.24	0.823	0.159	0.157	0.1	0.378	0.69	10.2	8.59	6.39	24.27	44.33
8		1839.93	1854.25	14.33	11.28	0.787	0.142	0.405	0.354	0.233	0.835	1.6	0.95	3.99	2.63	9.41
9		1854.25	1887.17	32.92	25.83	0.785	0.168	0.127	0.096	0.481	0.659	4.35	3.8	2.49	12.41	17.03
	All Zones	172.97	1887.17	1714.19	1617.72	0.944	0.253	0.254	0.177	12834218	0.745	408.83	304.93	285.79	19026255	1104.84

Table (2): Pay Summary from the cut-off for Archie model

Simandoux method:

Tables (4)(5) represent reservoir and pay summary results from the Simandoux model. The model yields high results (S_{wavg}) but less than the Archie model. The application of these models demands a type of dispersed shale, low shaliness, and more saline reservoir (low R_w) as found in the literature review. This model demands dispersed shale resistivity which varies with saturation and it is more difficult to determine.

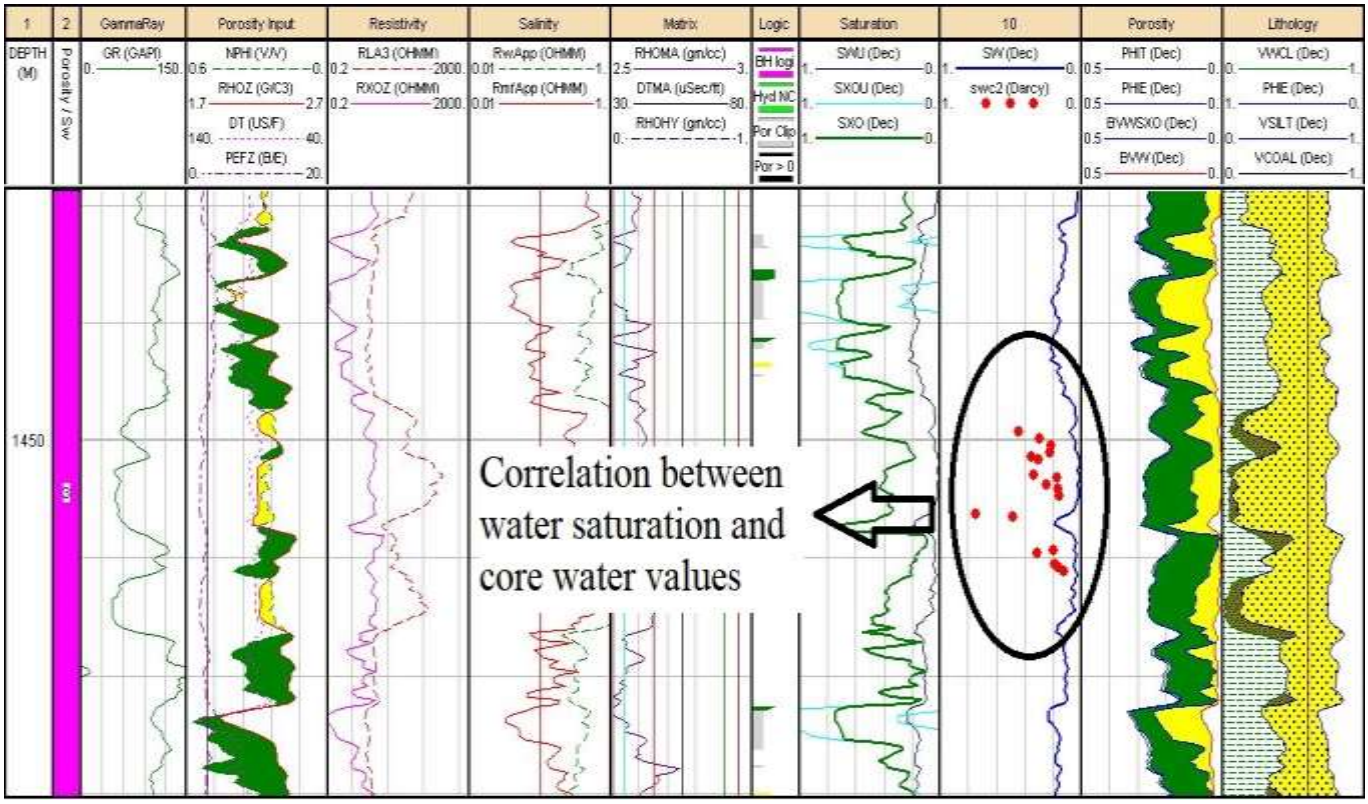

Figure (15): Correlation between water saturations with core water saturations values using Simandoux model

Reservoir Summary:

Zn #	Zone Name	Top	Bottom	Gross	Net	N/G	Av Phi	Av Sw	Av Vcl Ari	Av perm Ari	Av SXO Ari	Phi*H	PhiSo*H	Vcl*H	perm*H	SXO*H
1		172.97	1301.65	1128.67	1115.8	0.989	0.272	0.202	0.175	149.163	0.595	303.12	241.77	194.81	166435.5	663.36
2		1301.65	1437.44	135.79	135.79	1	0.273	0.194	0.255	296.482	0.517	37.02	29.85	34.58	40258.97	70.22
3		1437.44	1473.56	36.12	36.12	1	0.246	0.117	0.272	26.045	0.418	8.88	7.84	9.81	940.7	15.1
4		1473.56	1563.32	89.76	87.17	0.971	0.195	0.064	0.194	6.147	0.354	17.01	15.91	16.94	535.82	30.85
5		1563.32	1575.82	12.5	12.5	1	0.186	0.12	0.335	1.78	0.266	2.32	2.04	4.18	22.24	3.32
6		1575.82	1761.9	186.08	145.77	0.783	0.169	0.112	0.13	1	0.495	24.57	21.82	19	145.72	72.09
7		1761.9	1839.93	78.03	63.93	0.819	0.155	0.079	0.099	0.322	0.547	9.92	9.14	6.36	20.59	34.94
8		1839.93	1854.25	14.33	12.04	0.84	0.136	0.103	0.35	0.186	0.137	1.64	1.47	4.22	2.25	1.65
9		1854.25	1887.17	32.92	25.37	0.771	0.167	0.078	0.095	0.439	0.522	4.23	3.9	2.42	11.13	13.24
	All Zones	172.97	1887.17	1714.2	1634.49	0.954	0.25	0.183	0.179	127.485	0.554	408.7	333.75	292.31	208372.9	904.77

Table (3): Reservoir summary from the cutoff for Simandoux model

Pay Summary:

Zn #	Zone Name	Top	Bottom	Gross	Net	N/G	Av Phi	Av Sw	Av Vcl Ari	Av perm Ari	Av SXO Ari	Phi*H	PhiSo*H	Vcl*H	perm*H	SXO*H
1		172.97	1301.65	1128.67	1100.1	0.975	0.272	0.193	0.171	150.972	0.589	299.34	241.51	188.65	166084.6	648.08
2		1301.65	1437.44	135.79	135.79	1	0.273	0.194	0.255	296.482	0.517	37.02	29.85	34.58	40258.97	70.22
3		1437.44	1473.56	36.12	36.12	1	0.246	0.117	0.272	26.045	0.418	8.88	7.84	9.81	940.7	15.1
4		1473.56	1563.32	89.76	87.17	0.971	0.195	0.064	0.194	6.147	0.354	17.01	15.91	16.94	535.82	30.85
5		1563.32	1575.82	12.5	12.5	1	0.186	0.12	0.335	1.78	0.266	2.32	2.04	4.18	22.24	3.32
6		1575.82	1761.9	186.08	145.77	0.783	0.169	0.112	0.13	1	0.495	24.57	21.82	19	145.72	72.09
7		1761.9	1839.93	78.03	63.93	0.819	0.155	0.079	0.099	0.322	0.547	9.92	9.14	6.36	20.59	34.94
8		1839.93	1854.25	14.33	12.04	0.84	0.136	0.103	0.35	0.186	0.137	1.64	1.47	4.22	2.25	1.65
9		1854.25	1887.17	32.92	25.37	0.771	0.167	0.078	0.095	0.439	0.522	4.23	3.9	2.42	11.13	13.24
	All Zones	172.97	1887.17	1714.2	1618.79	0.944	0.25	0.176	0.177	128.504	0.549	404.92	333.48	286.15	208022.1	889.49

Table (4): Pay Summary from the cut-off for Simandoux model

Indonesian method:

Tables (6)(7) show the reservoir and pay summaries results from the Indonesian model. The average S_w is relatively higher compared to that of the Archie and Simandoux models. The Indonesian model demands a relatively higher shale contents reservoir and fresh water reservoir for its effectiveness. Quantitative interpretation has shown that the well penetrates high shale content reservoir which makes the Indonesian model useful for the study. Since its S_{wavg} value is close to the core data it is considered that it is the most suitable model for this study.

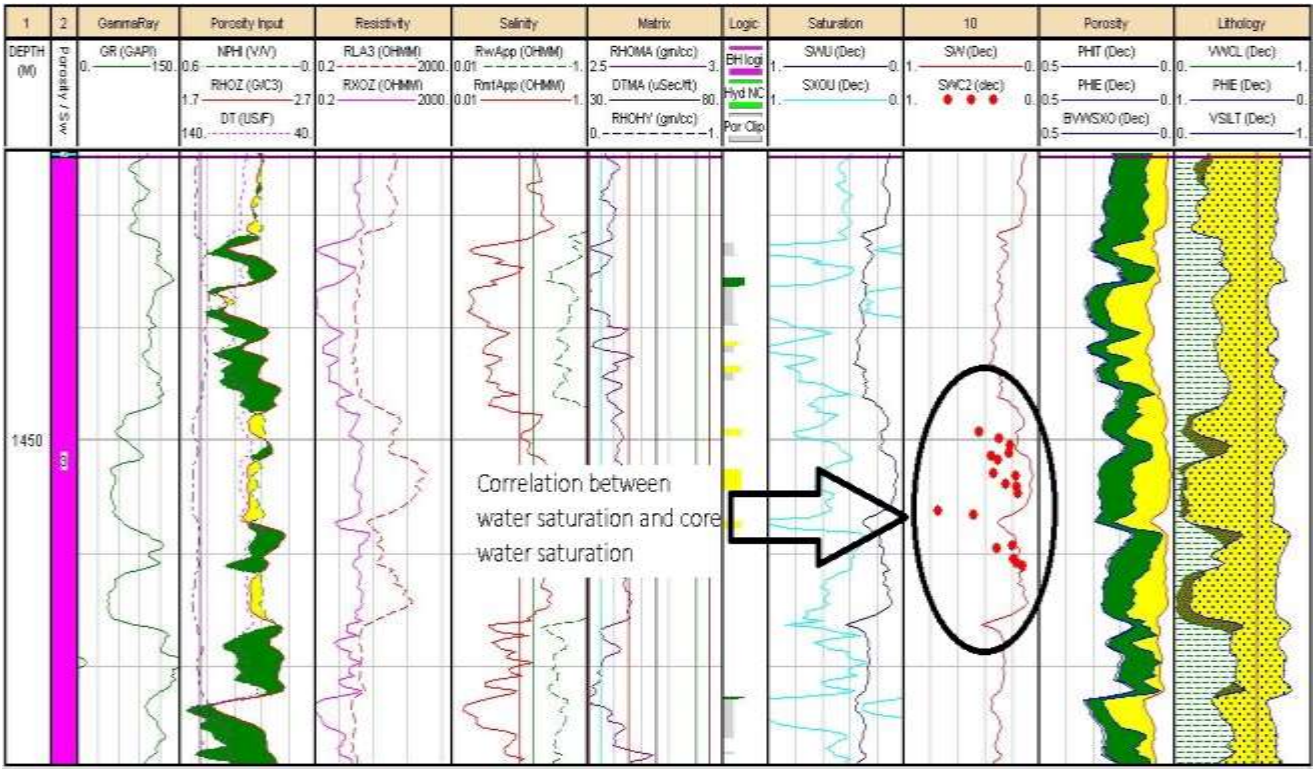

Figure (16): Correlation between water saturations with core water saturations values using Indonesian model

Reservoir Summary:

Zn	Zone Name	Top	Bottom	Gross	Net	N/G	Av Phi	Av Sw	Av Vcl	Av perm	Av SXO	Phi*H	PhiSo*H	Vcl*H	perm*H	SXO*H
#									Ari	Ari	Ari					
1		172.97	1301.64	1128.67	1115.79	0.989	0.274	0.327	0.175	157.387	0.719	305.56	205.74	194.81	175610.4	802.08
2		1301.65	1437.44	135.79	135.79	1	0.274	0.328	0.255	2.611	0.653	37.17	24.97	34.58	1.59	88.61
3		1437.44	1473.56	36.12	36.12	1	0.248	0.238	0.272	27.571	0.582	8.95	6.82	9.81	995.84	21.02
4		1473.56	1563.32	89.76	87.33	0.973	0.198	0.188	0.194	6.765	0.569	17.27	14.02	16.97	590.72	49.69
5		1563.32	1575.82	12.5	12.5	1	0.187	0.274	0.335	1.971	0.448	2.34	1.7	4.18	24.63	5.59
6		1575.82	1761.9	186.08	147.14	0.791	0.171	0.256	0.131	1.159	0.658	25.14	18.7	19.26	170.57	96.84
7		1761.9	1839.93	78.03	64.24	0.823	0.159	0.216	0.099	0.39	0.704	10.2	8	6.38	25.04	45.19
8		1839.93	1854.25	14.33	12.19	0.851	0.137	0.295	0.349	0.197	0.347	1.67	1.18	4.26	2.41	4.23
9		1854.25	1887.17	32.92	26.14	0.794	0.168	0.177	0.099	0.493	0.653	4.39	3.61	2.59	12.88	17.07
	All Zones	172.97	1887.17	1714.19	1637.23	0.955	0.252	0.31	0.179	118.128	0.69	412.68	284.73	292.85	177434	1130.34

Table (5): Reservoir summary from the cutoff for Indonesian model

Pay Summary:

Zn	Zone Name	Top	Bottom	Gross	Net	N/G	Av Phi	Av Sw	Av Vcl	Av perm	Av SXO	Phi*H	PhiSo*H	Vcl*H	perm*H	SXO*H
#									Ari	Ari	Ari					
1		172.97	1301.64	1128.67	1039.44	0.921	0.27	0.304	0.171	117.739	0.709	280.58	195.42	177.44	122382.1	736.57
2		1301.65	1437.44	135.79	135.33	0.997	0.274	0.328	0.255	2.611	0.652	37.09	24.93	34.56	1.59	88.2
3		1437.44	1473.56	36.12	36.12	1	0.248	0.238	0.272	27.571	0.582	8.95	6.82	9.81	995.84	21.02
4		1473.56	1563.32	89.76	87.02	0.969	0.198	0.187	0.194	6.786	0.568	17.21	14	16.9	590.56	49.45
5		1563.32	1575.82	12.5	12.5	1	0.187	0.274	0.335	1.971	0.448	2.34	1.7	4.18	24.63	5.59
6		1575.82	1761.9	186.08	145.47	0.782	0.171	0.254	0.132	1.172	0.656	24.93	18.6	19.19	170.46	95.36
7		1761.9	1839.93	78.03	63.7	0.816	0.159	0.214	0.1	0.393	0.702	10.14	7.97	6.37	25.02	44.72
8		1839.93	1854.25	14.33	12.12	0.846	0.137	0.293	0.351	0.198	0.343	1.66	1.17	4.25	2.4	4.16
9		1854.25	1887.17	32.92	26.14	0.794	0.168	0.177	0.099	0.493	0.653	4.39	3.61	2.59	12.88	17.07
	All Zones	172.97	1887.17	1714.19	1557.82	0.909	0.249	0.292	0.177	87.278	0.682	387.28	274.22	275.3	124205.5	1062.15

Table (6): Pay Summary from the cut-off for Indonesian model

4.7 Hydrocarbon Movability Index (Sw/Sxo):

Hydrocarbon movability index has been calculated from the optimistic Indonesian model and the value for zone 6 was **(0.611).** This value indicates that the hydrocarbon in this zone is movable**.**

CHAPTER 5

Conclusion and Recommendations:

The interpretation of lithology from GR, resistivity and Neutron-Density log have confirmed that the Bentiu and Aradeiba Formations consists of sands and few amount of shale (shaly sand formation).

The three models (Archie, Indonesian and Simandoux) were carried on and by comparing the water saturation values with the core data of Jake-South S2, the value from Indonesian model yields good matching. Therefore, the Indonesian method is found the most optimistic model for the shaly sand formations.

The calculated permeability was correlated with the core permeability model indicating that the technique of deriving the equation from the permeability and porosity cross plot is practical.

The oil saturation derived from the **equation (3.10.10)** is needed to calculate the hydrocarbon mobility index. This index is used to determine the movable hydrocarbon of the pay zones, in order to detect the commercial and signature hydrocarbon zone to be further introduced to the production stage.

It is recommended that all water saturation interpretation models results should be checked against water analysis results from core data, to confirm the accuracy of the methodology and work flow.

It is also recommended that model parameters (**a, m, n**, $\mathbf{R_w}$, and $\mathbf{R_{sh}}$) should be delivered from laboratory measurements to reduce the uncertainties associated with them.

We recommended that in well S-2 at the Bentiu formation from the top depth 1434.0 to bottom depth 1640.0 we have subzones that are divided into primary zones and secondary zones according to the values of oil and water saturation, porosity and permeability.

Primary zones:

- At the depth from 1504m to 1510m we found that the values of S_W range between (7% - 13%), calculated permeability (21.6 – 35) and effective porosity (26% - 28%).

- At the depth from 1519m to 1524m the values of S_W range between (10% - 23.8%), calculated permeability (17.7– 23) Darcy, effective porosity (24% - 26%).
- At the depth from 1575m to 1590m we found that the values of S_W range between (20% - 38%), calculated permeability (2.8– 9) Darcy, effective porosity (23% - 24%).

Secondary zones:

- At the depth from1475m to 1490m the values of S_W range between (9% -12%), calculated permeability (2.41 – 15.5) Darcy and effective porosity (21% - 26.3%).
- At the depth from 1553m to 1563m the values of S_W range between (14% - 12%), , calculated permeability (0.4– 1) Darcy, effective porosity (15% - 24%).
- At the depth from 1606m to 1610m the values of S_W range between (21% - 25%), calculated permeability (7– 13) Darcy, effective porosity (13% - 22%).

Its recommended in these zones that yield good results of movable oil to be considered for well testing stage and after that well completion can be undertaken.

References:

Abdelhakam E. Mohamed and Ali Sayed Mohammed (2008). Stratigraphy and tectonic evolution of the oil producing horizons of Muglad basin, Sudan.

Adeoti, L., et al. (2009). An integrated approach to volume of shale analysis: Niger Delta example, Offrire Field. World Applied Sciences Journal 7(4): 448452.

Alfosail, K. and A. Alkaabi (1997). Water saturation in shaly formation. Middle East Oil Show and Conference, Society of Petroleum Engineers.

Bhuyan, K. and Q. Passey (1994). Clay estimation from GR and neutron-density porosity logs. SPWLA 35th Annual Logging Symposium, Society of Petrophysicists and Well-Log Analysts.

Bhuyan, K. and Q. Passey (1994). Clay estimation from GR and neutron-density porosity logs. SPWLA 35th Annual Logging Symposium, Society of Petrophysicists and Well-Log Analysts.

Coates, G. R. and J. L. Dumanoir (1973). A new approach to improved log-derived permeability. SPWLA 14th Annual Logging Symposium, Society of Petrophysicists and Well-Log Analysts.

Darling, T. (2005). Well logging and formation evaluation, Elsevier.

Dalland, A., Wosrsley, D, & Ofstad, K. (1988). Astratigraphic scheme for the Mesozoic and Cenozoic succession offshore Norway north 62 N. NPD Bull, 4,67.

David, S. O., et al. (2015). A Universal Equation to Calculate Shale Volume for Shaly-Sands and Carbonate Reservoirs. SPE Latin American and Caribbean Petroleum Engineering Conference, Society of Petroleum Engineers.

De Waal, J. (1989). Influence of clay distribution on shaly sand conductivity. SPE Formation Evaluation 4(03): 377-383.

Doré, A. (1995). Barents Sea geology, petroleum resources and commercial potential. Arctic: 207-221.

Doveton, J. (2001). All models are wrong, but some models are useful:"solving" the Simandoux equation. Kansas Geological Survey, University of Kansas, Lawrence, Kansas USA.

Ellis, D. V., et al. (2004). Porosity from neutron logs II: interpretation. Petrophysics 45(01).

Ellis, D. V. and J. M. Singer (2007).

Ferns, T. W. (2000). Petrophysical properties from small samples using image analysis techniques. TU Delft, Delft University of Technology.

Fertl, W. and G. V. Chilingar (1988). Determination of volume, type, and distribution modes of clay minerals from well logging data. SPE Formation Damage Control Symposium, Society of Petroleum Engineers.

Fertl, W. H. and G. W. Hammack (1971). A comparative look at water saturation computations in shaly pay sands. SPWLA 12th Annual Logging Symposium, Society of Petrophysicists and Well-Log Analysts.

Fleury, M., et al. (2004). Evaluation of water saturation from resistivity in a carbonate field. From laboratory to logs. Proceedings of International Symposium of the Society of Core Analysts, Abu Dhabi, UAE.

Freedman, R., et al. (1998). Combining NMR and density logs for petrophysical analysis in gas-bearing formations. SPWLA 39th Annual Logging Symposium, Society of Petrophysicists and Well-Log Analysts.

Gaymard, R. and A. Poupon (1968). Response of neutron and formation density logs in hydrocarbon bearing formations. The Log Analyst 9(05). Gimbe, M. P. S. (2015). Formation Evaluation and Uncertainty Analysis of the Ormen Lange Field, Norwegian Sea offshore Norway.

Hamada, G. and M. N. Al-Awad (2000). Petrophysical evaluation of low resistivity sandstone reservoirs. Journal of Canadian Petroleum Technology 39(07).

Hermanrud, C., et al. (2014). Petroleum column-height controls in the western Hammerfest Basin, Barents Sea. Petroleum Geoscience 20(3): 227-240.

Hill, H., et al. (1979). Bound Water In Shaly Sands-Its Relation To Q And Other Formation Properties. The Log Analyst 20(03)

Thomas J. Schull (1988) Rift Basins of interior Sudan.

Zaki Bassiouni (1994) Theory, measurements and interpretation of well log.